Title: Targeting islet PTP1B improves islet graft revascularization and transplant outcomes

Authors: Hugo Figueiredo[1,2,3], Ana Lucia C. Figueroa[1,2], Ainhoa Garcia[1,4], Rebeca Fernandez-Ruiz[1,4], Christophe Broca[5], Anne Wojtusciszyn[5,6,7], Rita Malpique[1], Rosa Gasa[1,4]*, Ramon Gomis[1,2,4,8,9]*

Affiliations:

[1]Diabetes and Obesity Research Laboratory, August Pi i Sunyer Biomedical Research Institute (IDIBAPS), 08036 Barcelona, Spain.

[2]University of Barcelona, 08036 Barcelona, Spain.

[3] Escuela de Medicina y Ciencias de la Salud, Dept. Medicina Cardiovascular y Metabolómica, Tecnológico de Monterrey, 66278 San Pedro Garza García, Nuevo León, Mexico.

[4]Centro de Investigación Biomédica en Red de Diabetes y Enfermedades Metabólicas Asociadas (CIBERDEM), 28029 Madrid, Spain.

[5] CHU Montpellier, Laboratory of Cell Therapy for Diabetes (LTCD), Hospital St-Eloi, 34295 Montpellier, France.

[6] Department of Endocrinology, Diabetes and Nutrition, University Hospital of Montpellier, Lapeyronie Hospital, 34295 Montpellier, France.

[7] Service of Endocrinology, Diabetes and Metabolism, Lausanne University Hospital, 1011 Lausanne, Switzerland

[8] Universitat Oberta de Catalunya (UOC), 08018 Barcelona

[9] Department of Endocrinology and Nutrition, Hospital Clinic of Barcelona, 08036 Barcelona, Spain.

*Corresponding author. Email: RGASA@clinic.cat (R. Gasa); ramon.gomis@idibaps.org (R. Gomis)

One Sentence Summary: Inhibition of tyrosine phosphatase PTP1B in mouse and human islets promotes islet revascularization and improves graft survival and function.

OVERLINE: ISLET TRANSPLANTATION

Abstract:

Deficient vascularization is a major driver of early islet graft loss and one of the primary reasons for the failure of islet transplantation as a viable treatment for type 1 diabetes. This study identifies the protein tyrosine phosphatase 1B (PTP1B) as a potential modulator of islet graft revascularization. We demonstrate that grafts of pancreatic islets lacking PTP1B exhibit increased revascularization, which is accompanied by improved graft survival and function, and recovery of normoglycemia and glucose tolerance in diabetic mice transplanted with PTP1B-deficient islets. Mechanistically, we show that the absence of PTP1B leads to activation of Hypoxia-inducible factor 1-alpha (HIF1α)-independent Peroxisome proliferator-activator receptor gamma co-activator 1alpha (PGC1α)/ Estrogen related receptor alpha (ERRα) signaling and enhanced expression and production of Vascular endothelial growth factor A (VEGF-A) by ß-cells. These observations were reproduced in human islets. Together, these findings reveal that PTP1B regulates islet VEGF-A production and suggest that this phosphatase could be targeted to improve islet transplantation outcomes.

Introduction

One of the main clinical problems related to pancreatic islet transplantation is incomplete graft revascularization, which impairs oxygen and nutrient delivery and hormone and secretagogue modulation *(1–3)*. These deficiencies contribute toward the primary failure of transplanted islets *(4, 5)*. The native islet architecture is characterized by an ultra-dense capillary network responsible for the delivery of oxygen, hormones, and nutrients to islet cells and the efficient dispersal of islet hormones into the bloodstream *(6)*. During isolation, islets are severed from their native vascular network *(7)*; thus, after transplantation, the survival and function of islet grafts depend on the re-establishment of vessels within the grafts to derive blood flow from the host vascular system *(5, 8–11)*.

Intra-islet endothelial cells (IECs) participate in the early stages of angiogenesis and vasculogenesis, however the exact role IECs have in improving revascularization outcomes is still unclear *(12–14)*. Although the molecular mechanisms underlying islet revascularization remain elusive, numerous factors have been implicated, such as vascular endothelial growth factor A (VEGF-A), a key angiogenic molecule that stimulates extraembryonic blood vessel formation *(15, 16)*. Previous therapies aimed at inducing VEGF-A expression in islets have resulted in the hypervascularization of the islet, compromising islet architecture and inducing the loss of ß-cell mass *(17–19)*. VEGF-A is expressed and secreted in response to hypoxia through the activation of the hypoxia-inducible factor (HIF) signaling cascade *(20, 21)*, or in response to nutrient deprivation or ischemia by the upregulation of the peroxisome proliferator-activated receptor gamma coactivator 1alpha (PGC1α)*(22)*. The induction of VEGF-A by PGC1α does not involve the canonical hypoxia response pathway or HIF *(22)*. Instead, PGC1α coactivates the orphan nuclear receptor ERRα (estrogen-related receptor alpha) *(22, 23)*. ERRα is known to

interact physically and functionally with PGC1α and is involved in the activation of fatty acid oxidation and oxidative phosphorylation *(22, 24)*.

The protein tyrosine phosphatase 1B (PTP1B) regulates phosphotyrosine signaling in several intracellular transduction pathways involved in cell growth, differentiation, metabolism, apoptosis and gene transcription *(25)*. In endothelial cells (ECs), tyrosine phosphorylation of both the VEGF type II receptor (VEGFR2) and the adhesion molecule VE-CADHERIN (vascular endothelial cadherin) constitutes an important branch of the signaling events by which VEGF-A stimulates angiogenesis and vasculogenesis *(26–28)*. PTP1B has been shown to inhibit phosphorylation of both proteins, thus negatively affecting these processes *(27)*. However, the role of PTP1B in islet graft revascularization has not been previously described.

Results

Deletion of PTP1B in pancreatic islets decreases the rate of endothelial cell loss in vitro.

We sought to investigate endothelial cell content in pancreatic islets from constitutive PTP1B knockout ($PTP1B^{-/-}$) mice. Immunofluorescence staining of the EC marker PECAM-1 in freshly isolated islets and in islets cultured for two days [IECs are lost with culture *(14)*] revealed that the $PECAM^{+}$ area was similar in freshly isolated $PTP1B^{-/-}$ and $PTP1B^{+/+}$ islets (Fig. 1A,B). However, after two days of culture, $PTP1B^{-/-}$ islets exhibited three-fold higher $PECAM^{+}$ area than $PTP1B^{+/+}$ islets (Fig. 1A,B), suggesting increased IEC content in $PTP1B^{-/-}$ islets. To corroborate this observation, we quantified expression of genes encoding EC markers PECAM-1 (*Pecam1*), VEGFR2 (*Kdr*), and VE-CADHERIN (*Cdh5*). These genes were all upregulated in cultured $PTP1B^{-/-}$ islets relative to $PTP1B^{+/+}$ islets (Fig. 1C).

Because PTP1B has been previously shown to modulate apoptosis and insulin secretion in ß-cell lines and freshly isolated mouse islets *(29–31)*, we evaluated whether these processes were affected in PTP1B$^{-/-}$ islets. We found similar *Caspase3* and *Caspase9* transcript expression and a comparable number of cleaved-CASPASE3^{+} cells between two-day cultured PTP1B$^{-/-}$ and PTP1B$^{+/+}$ islets (Fig. 1D-F). Similarly, we found no differences in glucose-induced insulin secretion and islet insulin content between genotypes (fig. S1). Together, these observations reveal that PTP1B$^{-/-}$ islets present reduced loss of IECs in culture without apparent alterations in cell survival or insulin secretion.

Transplanted PTP1B$^{-/-}$ islets restore normoglycemia and circulating insulin concentration in diabetic mice.

To study the effect of PTP1B loss on the engraftment of islets, we performed a suboptimal allotransplantation of two-day cultured PTP1B$^{-/-}$ or PTP1B$^{+/+}$ islets into the anterior chamber of the eye of streptozotocin (STZ)-treated diabetic BALB/c mice (Fig. 2A). The anterior chamber of the eye is a privileged transplantation site, enabling non-invasive in vivo imaging *(32, 33)*, fast islet engraftment by blood vessels of the host iris (a highly vascular site) *(34–36)*, and reduced graft early rejection sustained by ocular immune privilege that suppresses immune cell proliferation and purge of the immune cells that enter the eye *(37)*. One week after STZ administration, 85% of the mice presented an average blood glucose of 340 mg/dL; no mice recovered spontaneously from STZ-induced diabetes. STZ-treated diabetic mice were randomly organized into three groups: transplanted with PTP1B$^{-/-}$ islets (PTP1B$^{-/-}$tx$^{balb\text{-}stz}$), transplanted with PTP1B$^{+/+}$ islets (PTP1B$^{+/+}$tx$^{balb\text{-}stz}$), or left untransplanted (non-transplanted). A fourth group of non-diabetic BALB/c mice was monitored in parallel and used to establish normoglycemia

threshold. Each transplanted mouse received 200 islets and was monitored for 28 days. Mice in the PTP1B$^{-/-}$tx$^{balb\text{-}stz}$ group showed a reduction in blood glucose concentration and achieved normoglycemia by day 21 (Fig. 2B). By contrast, the PTP1B$^{+/+}$tx$^{balb\text{-}stz}$ and non-transplanted groups exhibited no recovery in non-fasting glycemia (Fig. 2B). All STZ-induced diabetic mice presented with an initial decrease in body weight, due to the effects of STZ (Fig. 2C). However, following transplantation, the PTP1B$^{-/-}$tx$^{balb\text{-}stz}$ group recovered and gained body weight until the end of the experiment (Fig. 2C). The other two diabetic groups did not recover their initial body weight (Fig. 2C).

To assess graft function, we performed an IPGTT (intraperitoneal glucose tolerance test) on day 28. Results showed that the PTP1B$^{-/-}$tx$^{balb\text{-}stz}$ group presented comparable glucose tolerance to non-diabetic mice, whereas the PTP1B$^{+/+}$tx$^{balb\text{-}stz}$ and non-transplanted groups exhibited severe glucose intolerance (Fig. 2D,E). Supporting these findings, plasma insulin concentration was similarly increased after the glucose bolus in PTP1B$^{-/-}$tx$^{balb\text{-}stz}$ and non-diabetic groups, whereas the PTP1B$^{+/+}$tx$^{balb\text{-}stz}$ and non-transplanted groups lacked glucose responsiveness (Fig. 2F). At the end of the follow-up period we harvested pancreata to measure insulin content. All STZ-treated groups, regardless of the type of transplanted islets, presented an average 10-15% remaining insulin content compared to non-diabetic mice (Fig. 2G), thus supporting that amelioration of glucose homeostasis in the PTP1B$^{-/-}$tx$^{balb\text{-}stz}$ group originates from the islets transplanted in the eye.

PTP1B$^{-/-}$ islet grafts exhibit improved revascularization and survival.

We next investigated revascularization of the islet grafts transplanted in the eye. We assessed in vivo graft functional revascularization seven, fifteen and 28 days after transplantation, using two-

photon microscopy after injection of rhodamine B isothiocyanate (RITC)-dextran (Fig. 3A). In agreement with other studies *(2, 38)*, we found that vascular density reached its maximum 15 days after transplant in both experimental groups (Figure 3B). Nonetheless, $PTP1B^{-/-}tx^{balb\text{-}stz}$ grafts presented approximately 1.5-fold higher vascular density than $PTP1B^{+/+}tx^{balb\text{-}stz}$ grafts at all times studied (Fig. 3B). Likewise, the percentage of vascular area was also maximum at day 15 in both groups, and $PTP1B^{-/-}tx^{balb\text{-}stz}$ grafts presented a two-fold greater vascular area than $PTP1B^{+/+}tx^{balb\text{-}stz}$ at all times (Fig. 3C).

To study graft survival, we assessed in vivo cell death after propidium iodide (PI) injection and apoptosis by cleaved-CASPASE3$^+$ immunofluorescence in paraffin sections of the engrafted eyes. Results revealed a significant decrease in the percentage of PI$^+$ nuclei ($P < 0.001$, Fig. 3A,D) and of cleaved-CASPASE3$^+$ cells ($P < 0.01$, Fig. 3E,F) in $PTP1B^{-/-}tx^{balb\text{-}stz}$ grafts when compared with $PTP1B^{+/+}tx^{balb\text{-}stz}$ grafts. Lastly, we measured insulin positive area in engrafted eyes and found that, on average, 76% of $PTP1B^{-/-}tx^{balb\text{-}stz}$ graft cells were ß-cells as compared to 69 % in the $PTP1B^{+/+}tx^{balb\text{-}stz}$ graft (Fig. 3E,G). In sum, these data demonstrate that transplanted $PTP1B^{-/-}$ islets exhibit improved vascularization and cell survival as compared with control islets.

IECs are not responsible for improved revascularization of $PTP1B^{-/-}$ islet grafts

Because IECs are known to participate in the early stages of graft revascularization *(12, 39–41)*, we examined their involvement in improved vascularization of $PTP1B^{-/-}tx^{balb\text{-}stz}$ islet grafts. We depleted the IEC population from the islets to be transplanted by maintaining them in culture for several days *(14)*. $PTP1B^{-/-}$ islets presented a lower rate of IEC loss than $PTP1B^{+/+}$ islets (Fig 4A,B). Yet, by day seven, we were not able to detect any PECAM$^+$ cells in either $PTP1B^{-/-}$ or

PTP1B$^{+/+}$ islets (Fig. 4B). These results were validated at the gene expression level (fig. S2A). Therefore, PTP1B$^{-/-}$ and PTP1B$^{+/+}$ islets cultured for seven days were considered to be free of IECs. Further, islets from both genotypes exhibited comparable glucose-induced insulin secretion (fig. S2B) and showed similar expression of the apoptotic genes *Caspase3* and *Caspase9* (fig. S2C). Confirming the lack of endothelial cells, vestigial expression of the endothelial markers, *Pecam1*, *Kdr,* and *Cdh5*, was detected, but no differences were observed between genotypes (fig. S2D).

We then transplanted a suboptimal number of IEC-depleted islets into the anterior chamber of the eye of STZ-treated diabetic BALB/c mice and followed them for 28 days. Mice transplanted with IEC-depleted PTP1B$^{-/-}$islets (PTP1B$^{-/-}$EC$^{\varnothing}$tx$^{balb\text{-}stz}$) achieved normoglycemia seven days after transplant, whereas IEC-depleted PTP1B$^{+/+}$islets (PTP1B$^{+/+}$EC$^{\varnothing}$tx$^{balb\text{-}stz}$) did not normalize glycemia (Fig. 4C). Moreover, PTP1B$^{-/-}$EC$^{\varnothing}$tx$^{balb\text{-}stz}$ mice recovered and continued gaining weight until day 28 whereas PTP1B$^{+/+}$EC$^{\varnothing}$tx$^{balb\text{-}stz}$ mice did not gain any weight during the follow-up period (Fig. 4D). Immunofluorescence staining detected a 4.2-fold increase in PECAM-1^{+} area in the PTP1B$^{-/-}$EC$^{\varnothing}$tx$^{balb\text{-}stz}$ grafts when compared with the PTP1B$^{+/+}$EC$^{\varnothing}$tx$^{balb\text{-}stz}$ grafts (Fig. 4E,F). In addition, PTP1B$^{-/-}$EC$^{\varnothing}$tx$^{balb\text{-}stz}$ grafts showed a 61% decrease in cleaved CASPASE3^{+} cells when compared with PTP1B$^{+/+}$EC$^{\varnothing}$tx$^{balb\text{-}stz}$ (Fig. 4E,G). Together, these results support the notion that donor IECs are not responsible for improved graft revascularization in the absence of PTP1B.

Cultured and transplanted PTP1B$^{-/-}$ islets exhibit enhanced VEGF-A production

To mechanistically understand the increase in revascularization in the PTP1B$^{-/-}$tx$^{balb\text{-}stz}$ grafts, we initially investigated the expression of VEGF-A, a cytokine produced by islet cells which is known to be the principal inducer of angiogenesis *(11, 15)*. Immunofluorescence analysis of paraffin sections of the engrafted eyes using antibodies against VEGF-A and Insulin demonstrated that 89% of ß-cells in PTP1B$^{-/-}$tx$^{balb\text{-}stz}$ grafts expressed VEGF-A, whereas 35% expressed VEGF-A in the PTP1B$^{+/+}$tx$^{balb\text{-}stz}$ grafts (Fig. 5A,B), thus suggesting that enhanced VEGF-A production may underlie increased vascular network formation in PTP1B$^{-/-}$tx$^{balb\text{-}stz}$ islet grafts. Analysis of Insulin/VEGF-A co-staining revealed that, in both type of grafts, 90% of the cells expressing VEGF-A were ß-cells (Fig. 5A).

To understand why PTP1B$^{-/-}$ islet grafts exhibited higher VEGF-A expression, we studied *Vegfa* gene expression, VEGF-A protein content, and VEGF-A secretion by PTP1B$^{-/-}$ and PTP1B$^{+/+}$ islets cultured for two days (the conditions under which they were transplanted in Figs. 2-3). We found that *Vegfa* transcript levels were 3.9-fold higher in PTP1B$^{-/-}$ islets relative to controls (Fig. 5C). In agreement with increased gene expression, immunofluorescence analysis revealed that 92% of ß-cells from PTP1B$^{-/-}$ islets were positive for VEGF-A as compared to <25% of ß-cells in control islets (Fig. 5D,E). PTP1B$^{-/-}$ islets also exhibited augmented VEGF-A fractional secretion (relative to content) versus PTP1B$^{+/+}$ islets (Fig. 5F). Immunofluorescence analysis of VEGF-A expression in pancreata from PTP1B$^{+/+}$ and PTP1B$^{-/-}$ mice showed marginal VEGF-A staining in islets in both genotypes (fig. S3), supporting that native PTP1B$^{-/-}$ islets do not express more VEGF-A, and that islet VEGF-A production is potentiated after culture.

PTP1B$^{-/-}$ islets present activation of the PGC1α/ERRα axis

Based on prior findings *(20–22)*, we reasoned that the increase in VEGF-A production in two-day cultured PTP1B$^{-/-}$ islets might be due to enhanced hypoxia. However, we found no differences in *Hif1a* gene expression in knockout relative to control islets (Fig. 5G), thus indicating that HIF1α is unlikely to be responsible for upregulated *Vegfa* expression in PTP1B$^{-/-}$ islets. Instead, we observed upregulation of *Ppargc1a* (encoding PGC1α) and *Esrra* (encoding ERRα) (Figure 5G), revealing a possible modulation of the PGC1α/ERRα pathway by PTP1B. These results were validated at the protein level using immunoblot analysis (Fig. 5H).

Because the genes encoding PGC1α/ERRα and VEGF-A are normally induced by nutrient deprivation *(22)*, we sought to examine the ability of PTP1B to modulate this regulation. We cultured PTP1B$^{+/+}$and PTP1B$^{-/-}$ islets for two days in standard complete medium or in Hank's balanced salt solution (Hbss) to mimic nutrient deprivation. Islets cultured in Hbss showed increased *Ppargc1a* and *Esrra* mRNA as compared to islets cultured in complete medium, irrespective of the presence or absence of PTP1B (Fig. 5I,J). However, *Vegfa* mRNA was only significantly induced by Hbss culture in PTP1B$^{-/-}$ islets ($P < 0.001$, Fig. 5J). Because gene responses to nutrient deprivation were larger in PTP1B$^{-/-}$ than in PTP1B$^{+/+}$ islets, transcript levels for these genes were higher in nutrient-deprived PTP1B$^{-/-}$ islets relative to nutrient-deprived PTP1B$^{+/+}$ islets (Fig. 5K). Note that no difference was observed between PTP1B$^{+/+}$ and PTP1B$^{-/-}$ islets regarding *Hif1a* expression, supporting that nutrient deprivation does not activate this gene (Fig. 5K). Lastly, we measured VEGF-A secretion and confirmed that PTP1B$^{-/-}$ islets secreted more VEGF-A than PTP1B$^{+/+}$ islets under normal and nutrient deprivation conditions (Fig. 5L). VEGF-A secretion by PTP1B$^{-/-}$ islets was increased by nutrient deprivation whereas that of PTP1B$^{+/+}$ islets did not vary (Fig. 5L). Together, these results point to PGC1α, not HIF1α, as the likely mediator of the effects of PTP1B loss on *Vegfa* expression.

Silencing PTP1B in human islets induces VEGF-A expression and improves graft revascularization

We next asked whether the regulation of VEGF-A by PTP1B was conserved in human islets and, if so, whether loss of PTP1B improved vascularization of human islet grafts. We obtained five different human islet preparations with an average purity of 95.5% (± 1.3%) as assessed by dithizone staining, and a mean viability of 85.0% (±7.5%) as assessed by a carboxyfluorescein diacetate succinimidyl ester (CFDA)/PI staining (fig. S4).

We used RNA interference to reduce PTP1B in human islets. In a preliminary experiment we evaluated the uptake of a non-targeting fluorescence-labeled siRNA and confirmed strong green fluorescence in 52% to 87% of islet cells (fig. S5). We then used a pool of siRNAs against PTP1B (PTP1B-siRNA) and corroborated the reduction of PTP1B protein levels by immunoblot analysis (Fig. 6A) and by immunofluorescence staining (Fig. 6B) in islets transfected with PTP1B-siRNA relative to islets transfected with a non-targeting scrambled-siRNA. Quantification of $PTP1B^{+}$/$INSULIN^{+}$ cells revealed a 57% decrease in $PTP1B^{+}$ ß-cells in PTP1B-siRNA islets (Fig. 6C). Having validated the reduction in PTP1B protein content, we surveyed gene expression in two independent human islet batches (Fig. 6D). Two days after transfection, expression of the PTP1B gene (*PTPN1*) was reduced by 30% and 50%; *VEGFA* expression was up-regulated 1.4- and 3-fold; *PPARGC1A* expression 1.2- and 1.6-fold; and *ESRRA* expression 1.3- and 2.8-fold in islets treated with PTP1B-siRNA, as compared to scrambled-siRNA (Fig. 6D). By contrast, *HIF1A* mRNA levels remained unmodified (Fig. 6D). In agreement with activation of the *VEGFA* gene, PTP1B-silenced human islets exhibited six-fold higher VEGF-A secretion than islets transfected with the scrambled-siRNA (Fig. 6E).

After confirming enhanced production of VEGF-A, we investigated whether PTP1B inhibition improved revascularization of human islet grafts. To ensure silencing of PTP1B for longer duration (as required in transplantation experiments), we used lentiviral particles carrying shRNAs against PTP1B (sh-PTP1B LV). We first monitored infection efficiency by assessing GFP fluorescence (sh-PTP1B LV carries a CMV-driven tGFP) and observed abundant GFP+ cells two days after infection and fewer cells eight days post-infection (Fig. 6F). We then measured PTP1B protein content in whole islet extracts by immunoblot analysis and found that it was severely reduced two days after sh-PTP1B LV treatment but returned to control values (islets infected with sh-scrambled LV) by day eight (Fig. 6G). In agreement with PTP1B downregulation, VEGF-A secretion was 16-fold higher in sh-PTP1B LV islets as compared to sh-scrambled LV at day 2 (Fig. 6H). Despite VEGF-A secretion having decreased by 76% at day 8, VEGF release by sh-PTP1B LV islets remained higher than sh-scrambled LV islets (Fig. 6H). Finally, we transplanted 150 PTP1B-silenced or control human islets into the eyes of immunodeficient NSG mice (n=3 and n=2, respectively). Eight days after transplantation, grafts of sh-PTP1B LV islets presented improved functional vascularization compared to control grafts as measured by RITC-dextran and two-photon microscopy (Figure 6I). When contrasted against the in vitro results, sh-PTP1B LV islets maintained high expression of GFP eight days after implantation, suggesting that lentiviral expression was sustained longer in vivo than in vitro. These results confirm that inhibition of PTP1B induces VEGF-A production in human islets and improves revascularization of transplanted islets.

Discussion

Islet transplantation as a potential treatment for type 1 diabetes fails primarily due to poor survival of the islet grafts. Insufficient revascularization is mainly responsible for early graft loss and represents one of the major issues affecting long-term graft survival *(7, 39, 42)*. Searching for new targets to facilitate graft revascularization may lead to improved future outcomes in islet transplantation *(41)*.

Here we demonstrated that the absence of islet PTP1B increased graft functional vascularization by increasing the number of newly formed vessel branches and total graft vessel area. Several mechanisms could explain improved revascularization in PTP1B$^{-/-}$ islet grafts *(11, 14, 41)*. Because isolated PTP1B$^{-/-}$ islets show an upregulation of several EC markers as well as reduced IEC loss in culture, we considered the possibility that donor PTP1B$^{-/-}$ IECs contributed to the increased functional vasculature in grafts *(14, 41, 43)*. However, this hypothesis was refuted by our observation that mice transplanted with IEC-depleted PTP1B$^{-/-}$ islets still exhibited improved graft revascularization. Another possibility was that islets lacking PTP1B released more pro-angiogenic signals than control islets. Our finding that PTP1B$^{-/-}$ islet grafts expressed and secreted more VEGF-A, an angiogenic cytokine that stimulates extraembryonic blood vessel formation *(15, 16, 44)*, than control grafts favors this notion. One may suggest that a similar effect on revascularization could be obtained by using strategies to overexpress or directly administer VEGF-A to islets, as previously described *(17–19)*. However, these therapies induced hyper-revascularization of grafts associated with a loss of ß-cell mass and, consequently, impaired graft function. Thus, our approach differs from previous approaches and offers a major advantage, as we demonstrated that improved revascularization, by modulating endogenous VEGFA expression, was not associated with deleterious effects on ß-cell number or function in grafts.

Cells express and secrete VEGF-A in response to different stimuli, such as hypoxia *(43, 45–47)* and nutrient deprivation *(22)*. Our data showed that the upregulation of VEGF-A in islets lacking PTP1B was not associated with increased HIF1α, a major hypoxia sensor. A study conducted by Arany and colleagues *(22)* described that, in response to ischemia or nutrient deprivation, activation of VEGF-A could take place through HIF1-independent upregulation of PGC1α and coactivation of ERRα. Here we showed that PTP1B$^{-/-}$ islets had higher expression of *Ppargc1a* and *Esrra* mRNAs and their respective proteins, suggesting that this axis may be responsible for increased *Vegfa* expression. Downregulation of PTP1B had similar effects in human islets as in murine islets, which is in agreement with the predicted conservation of six out of 11 binding sites recognized by ERRα between the promoters of the mouse and human VEGF-A coding genes *(22)*. We also showed that the upregulation of PGC1α/ERRα in islets was enhanced in response to nutrient deprivation. In this regard, it is plausible to predict that, before maximum revascularization, islets transplanted into the anterior chamber of the eye are exposed to nutrient deprivation *(47–49)*; the aqueous humor of the eye that serves as the graft milieu, although capable of sensing blood plasma changes such as those in glucose, presents lower protein content than plasma *(50–52)*.

Based on all these data and data in previous published studies, we propose a model whereby VEGF-A expression is enhanced via the PGC1α/ERRα axis in transplanted PTP1B-/- islets (fig. S6). Briefly, under nutrient deprivation conditions, the absence or downregulation of PTP1B enhances the upregulation of the gene encoding PGC1α by mechanisms that remain to be elucidated. In turn, PGC1α increases the expression of the orphan nuclear receptor ERRα. It is known that PGC1α/ERRα dimers recognize and bind several conserved sites at the *Vegfa* gene promoter thus inducing the expression of this gene *(22–24)*. Enhanced *Vegfa* gene expression

results in an increase in both protein and secretion of VEGF-A by islets. Secreted VEGF-A will interact with its receptor, VEGFR2, in endothelial cells, activating the signaling pathway of angiogenesis towards the islets *(26, 27)*.

We propose that better graft revascularization contributes to enhanced survival and restoration of endogenous insulin production in recipients of PTP1B$^{-/-}$ islet grafts. However, because we used a loss-of-function genetic mouse model as islet donor, we cannot rule out that constitutive loss of PTP1B might have also influenced intrinsically the endurance and function of transplanted PTP1B$^{-/-}$ ß-cells in our study. In any case, if we contemplate the clinical translation of this strategy, we should aim at inhibiting PTP1B during a limited period of time, for example, at pre-implantation or early transplantation stages, when the proangiogenic effects of VEGF are required. In this scenario, the potential effects of PTP1B blockade on ß-cell physiology, if any, would be also temporary. In this regard, we found that ex vivo treatment of human islets with RNA interference approaches led to effective downregulation of PTP1B, increased VEGF-A production in vitro and enhanced early graft revascularization. Future studies will be required to fully evaluate the impact of transient PTP1B inhibition on long-term human islet graft function both in healthy and diabetic mouse models.

In conclusion, we demonstrate that loss or downregulation of PTP1B potentiates VEGF-A production in mouse and human islets and that this effect is associated with increased graft revascularization. Our results support the notion that PTP1B may represent a molecular target to improve islet graft revascularization. Our findings represent a proof-of-concept that could lead to improved future outcomes, eliminating an important stumbling block to islet transplantation as a means of effectively treating type 1 diabetes.

Materials and Methods

Study design

The primary objective of this study was to determine whether the absence or the downregulation of PTP1B improved islet graft revascularization and survival. In vivo studies were performed by transplanting islets into the anterior chamber of the eye of diabetic male mice. Animal handling and care procedures were fulfilled by Federation of European Laboratory Animal Science Associations (FELASA)-trained scientists and in accordance with the local ethics committee, the Spanish royal decree 214/1997 and the European Directive 2010/63/EU. We based our group sizes on power analysis to achieve 80% likelihood of detection with a type 1 error of 0.05, an effect size of 50% and a 30% standard deviation. All animals that underwent the diabetes induction protocol that presented glycemia below 250 mg/dL for three consecutive days or presented ≥ 20% weight loss were excluded from the study and euthanized. We did not use randomization or blinding approaches to allocate the remaining animals into the experimental groups. In vitro experiments were performed by randomly allocating isolated mouse islets (primary culture) into groups according to their genotype. Experiments involving human islets were performed in agreement with the local ethics committee (CHU, Montpellier) and the institutional ethical committee of the French Agence de la Biomédecine (DC Nos. 2014-2473 and 2016-2716). Informed consent was obtained for all donors. For each experiment, sample size reflects the number of independent biological replicates and is provided in the figure legend.

Animals

Animals were maintained on standard light/dark cycle; food and water were provided *ad libitum*. PTP1B transgenic mice (wild-type, $PTP1B^{+/+}$; knockout, $PTP1B^{-/-}$) were obtained from Abbot Laboratories *(53)*. Experiments were performed with eight- and nine-week-old male mice

littermates, maintaining the genetic background of 129/SvJxC57Bl6/J. Genotyping was performed as described in Supplementary Methods. Male BALB/c mice were acquired from Charles River Laboratories (London, England) at the age of six weeks and experiments were performed at age of eight weeks. Diabetes was induced in BALB/c mice by streptozotocin (STZ) *(54, 55)* as detailed in Supplementary Methods.

Isolation of mouse pancreatic islets and culture

Islets were isolated by standard procedures using collagenase digestion (Supplementary Methods). Isolated islets were cultured in RPMI 1640 medium (Sigma-Aldrich, Saint Louis, USA) containing 11 mM glucose, 0.3g/L L-glutamine, 2g/L $NaHCO_3$, 10% heat-inactivated fetal bovine serum (FBS, Hyclone, Logan, UT) and Penicillin-Streptomycin (100 units/ml penicillin, 100 pg/ml streptomycin) (GE Healthcare Life Sciences, PGH, USA). The islets were cultured at 37°C under a 5% CO_2 and 95% air-humidified atmosphere. Characterization of $PTP1B^{-/-}$ and $PTP1B^{+/+}$ islets (gene expression, immunohistochemistry, immunoblotting, and insulin secretion) was performed using two-day cultured islets. For transplantation experiments, islets were cultured for two days prior to implantation, where the first day was for islet recovery from isolation, and the following day for recovery from labeling protocol (see Islet labeling). As it is known that IECs decrease over time in culture *(14, 41),* $PTP1B^{-/-}$ and $PTP1B^{+/+}$ islets were cultured for seven days after isolation to eliminate IECs. The culture medium used was the same as used in standard culture and was changed every two days. Nutrient deprivation conditions *(22)* involved culturing islets, under 37°C, 5% CO_2 and 95% air-humidified atmosphere, for two days in Hank's balanced salt solution (Hbss; Sigma-Aldrich) with 2 g/L of glucose, 100 units/ml penicillin, and 100 pg/ml streptomycin.

Islet labeling and allotransplantation

Diabetic male BALB/c mice were transplanted with 200 islets isolated from $PTP1B^{-/-}$ or $PTP1B^{+/+}$ mice (suboptimal allotransplantation), in the anterior chamber of the eye. Before transplantation, islets were labeled with the long-term tracer for viable cells CFDA (Invitrogen, OR, USA), which passively diffuses through the membrane of viable cells and emits fluorescence after intracellular esterases cleave its acetate groups *(56)*. Islets were washed with Dulbecco's phosphate buffer saline (PBS; Sigma-Aldrich) with 0.1% bovine serum albumin (BSA) and then incubated at 37°C, in a 5% CO_2 and 95% air-humidified atmosphere for 15 minutes in a 10 μM CFDA SE- PBS/BSA dilution. CFDA-loaded islets were washed and cultured in standard media for one day before being transplanted. Transplantation was performed as described *(33)*. Detailed procedure is provided in Supplementary Methods.

Physiological studies: weight, glycemia and glucose tolerance test.

During the 28-day follow up period, weight and non-fasting blood glucose concentration were measured within the same schedule at the indicated days. Blood glucose was measured by collecting blood from the tail vein directly to the glucometer strap. Glucose tolerance test was performed after a six-hour fast. Mice were injected intraperitoneally with 2g/kg D-glucose. Blood glucose levels were measured 0, 15, 30, 60, 90 and 120 minutes after the injection; in-parallel blood was collected from the tail vein into a capillary blood collection system (Microvette, Sarstedt, Nümbrecht, Germany) to analyze plasma insulin concentration by ELISA (Mercodia, Uppsala, Sweden).

In vivo revascularization and cell death imaging

Functional graft revascularization and cell death were assessed in vivo, 7, 15 and 28 days after transplantation. Briefly, the animals were anesthetized intraperitoneally with a ketamine-xylazine mix (100 mg/kg and 7.5 mg/kg) and received an intravenous injection of a mix composed of 100

mg/kg of RITC-dextran, molecular weight 70 kDa (Sigma-Aldrich) to assess functional vasculature, 250 µg/Kg of PI (Invitrogen) to assess cell death and 12 mg/Kg of Hoechst 33258 (Invitrogen) as a nuclear marker. Anesthetized animals were transferred to the microscope stage with the operated eye positioned in a cover glass with a drop of carboxymethylcellulose sodium, in the direction of the objective (40x water immersion objective). A microscope incubator chamber maintained the adequate temperature. Images of the grafts were acquired every 0.23 µm in a length of 50 µm using a two-photon laser at 900 nm, with automated motion artifact correction (Leica SP5 TPLSM, Leica Microsystems, Wetzlar, Germany). Images were collected for posterior analysis with ImageJ software v1.50d (Wayne Rasband, NIH, USA). At the end of the experiment, animals were placed under supervision in a warm environment until full recovery or euthanized to perform enucleation of the eye for posterior immunohistochemistry analysis.

Immunofluorescence staining in paraffinized eye sections and in whole islets

Eyes containing the grafts were fixed overnight in 2% paraformaldehyde and then dehydrated with ethanol gradient, cleared with xylol and paraffin-embedded. 4 µm-thick eye sections 15µm apart underwent a standard immunohistochemistry-immunofluorescence (IHC-IF) method for paraffin sections. Images were acquired using a Leica DMR HC epifluorescence microscope (Leica Microsystems). IHC-IF of the whole islet was performed as described *(58)*. For each islet, optical section images starting at the peripheral cell layers were acquired using a Leica TCS SPE confocal microscope (Leica Microsystems). Images were taken every 5 µm (for PECAM-1 labelling) or 10 µm, for a total of 60 µm/islet, using a 40x oil immersion objective. The 405, 488, and 532 nm lasers were used, and settings were maintained unaltered between islets and conditions in each experiment. IF studies in whole islets offer several advantages over traditional

methods such as constructing a three-dimensional mapping of IECs networks by optically sectioning islets with a confocal microscope *(57)*. Primary antibodies used were: guinea pig anti-insulin (1:1000 dilution, Dako, Glostrup, Denmark), mouse anti-glucagon (1:100, Dako), rabbit anti-PECAM-1 (1:20, Abcam, Cambridge, UK); rabbit anti-VEGF-A (1:100, Abcam), rabbit anti-Cleaved Caspase-3 (1:400, Cell Signaling, MA, USA). As secondary antibodies: Alexa Fluor 555 anti-guinea pig, Alexa Fluor 555 anti-rabbit and Alexa Fluor 288 anti-mouse at 1:500 dilution, and Alexa Fluor 488 anti-rabbit at 1:250 dilution (Thermo Fisher Scientific, MA, USA) were used. Hoechst 33258 (1:500, Invitrogen) or an antifade mounting medium with Dapi (Thermo Fisher Scientific) were used to mark nuclei. Positively stained cells and pixel areas were quantified using ImageJ 1.50d software (NIH, USA).

RNA isolation and quantitative PCR analysis

Total RNA was extracted, reverse transcribed and mRNA expression quantified by quantitative real time PCR (qRT-PCR) as previously described *(31, 58)*. Gene expression was normalized against *Tbp* or *ACTB* as endogenous controls for mouse and human islets respectively. Results were expressed relative to expression in control samples (given arbitrarily the value of 1). Primer sequences are provided in Supplementary Methods.

Immunoblotting and VEGF-A secretion

To prepare whole cell extracts, islets were lysed in RIPA buffer (Tris 50 mmol/l, pH 7.5, EDTA 5 mmol/l, NaCl, 150 mmol/l, Triton X-100 1%, SDS 0.1%, sodium fluoride10 mmol/l, sodium deoxycholate) supplemented with phosphatase and protease inhibitor cocktails (Roche, Basel, Switzerland). Islet lysates were frozen and thawed twice in 3 cycles, followed by ultrasonication with 3 short burst cycles of the 30s at 20kHz (20 000 cycles/s). Nuclear extracts were obtained by bursting islets with a hypotonic buffer (HEPES 10 mM, KCl 10 mM, EDTA 0.1 mM, EGTA

0.1 mM, pH8), with NP40 0.05%. After centrifugation, the nuclear pellet was incubated with a hypertonic buffer (HEPES 20 mM, NaCl 400 mM, EDTA 10 mM, EGTA 10 mM, glycerol 20%) to obtain nuclear protein extracts. All protein extracts were stored at -80°C until analysis.

Protein was quantified with the Lowry protein assay kit (Bio-rad, Hercules, USA). A total of 20 µg of protein extract was used for each replicate. Proteins were separated in a precast 4%-15% gradient gel (Bio-rad) and transferred onto a PVDF membrane. The membranes were blocked for one hour with Tween-20 0.05% and non-fat dry milk 5%, and then incubated overnight at 4 °C with antibodies against HIF1α (1:1000, Abcam, band: 120 kDa), PGC1α (1:1000, Abcam, band: 92 (105) kDa), ERRα (1:1000, Thermo Scientific, band: 55 kDa) and PTP1B (1:500, Upstate biotechnologies, NY, USA, band: 49 kDa). LAMIN-B1 (1:1000, Cell Signaling, band 66 kDa) and αTUBULIN (1:1000, Cell Signaling, MA, USA, band: 52 kDa) were used as loading controls. Protein bands were visualized using the Pierce ECL western blot substrate (Thermo Fisher Scientific) and analyzed using Image J software 1.50a.

VEGF-A secretion was measured by culturing islets for 48 hours in complete medium without FBS supplementation or directly in nutrient deprivation conditions (Hbss). Islets and culture medium were collected. The protein content from the culture medium was concentrated by centrifugal ultrafiltration (3 kDa, Merck-Millipore, MA, USA). VEGF-A secretion and islet VEGF-A content were quantified by ELISA (Abcam).

In vitro insulin secretion and pancreas insulin content

In vitro glucose-induced insulin secretion was studied in separate batches of eight islets by static incubation assays as previously described *(59)*. To determine total pancreatic insulin content, the harvested pancreata were homogenized in acid alcohol and extracted overnight at 4˚C. The

solution was then centrifuged to remove tissue in suspension and neutralized. Insulin concentration was measured by ELISA (Mercodia).

Human islet isolation and culture

Human islets were obtained from five cadaveric donors (males and females) with an average age of 60 years (±12 years) and BMI of 28.8 kg/m^2 (±2.5 kg/m^2) (table S1). Isolated islets were prepared by collagenase digestion followed by density gradient purification at the Laboratory of Cell Therapy for Diabetes (Hospital Saint-Eloi, Montpellier, France), as previously described *(60)*. After reception, human islets were maintained in culture, for at least 3 days, using RPMI-1640 with 5.6 mM glucose, 10 % FBS and antibiotics. Assessment of batch purity and viability was performed as described in Supplementary Methods.

RNA interference

For in vitro experiments, PTP1B knockdown in human islets was achieved by transfection of a *PTPN1* SMART pool Accell siRNA (Dharmacon, CO, USA) following the manufacturer's instructions with minor modifications. Human islets were pre-incubated in a dilute solution of trypsin (50 mg/mL) for 1.5 minutes at 37°C to increase transfection efficiency. In a pilot experiment, diffusion of siRNA throughout the islets was evaluated 72 hours after transfection of a non-targeting Accell siRNA labelled with 6-FAM (Dharmacon) using confocal microscopy (laser 488nm) and bright field. Islet autofluorescence was also visualized and set as a negative control, using the same excitation and emission settings for FAM-siRNA assessment (517 nm). Optical sections, 10µm apart, were acquired and analyzed using Image J 1.50a. Following a three-day culture with siRNA, the islets were collected and RNA and protein extracted as described previously. Gene expression was assessed by qRT-PCR, and protein content was assessed by immunoblotting.

For transplantation experiments, lentiviral particles carrying short hairpin (sh) RNAs were used as this strategy sustains better the downregulation of a gene in islets *(61–63)*, without affecting islet function *(61–63)* when compared with siRNA transfection. A pool of four independent lentiviruses carrying unique shRNAs specific for human PTP1B (sh-PTP1B LV) and the control lentivirus carrying a non-specific scrambled shRNA (sh-scrambled LV) were acquired from OriGene Technologies (Rockville, USA). In addition to the shRNA, all lentiviruses carried a CMV-driven tGFP to monitor transduction efficiency. Human islets were pelleted at 50 x g for two minutes and then incubated with 1000 µl of trypsin (250 mg/L)-EDTA (0.48 mM) solution for three minutes in a cell culture incubator (37ºC, 5% CO_2). The islet suspension was carefully pipetted up and down. After adding 1000 µl of complete RPMI (1g/L glucose, 10% FBS, pen-strep) islets were pelleted by centrifugation at 100 x g for one minute. Batches of 150 islets were then resuspended in serum free RPMI (final volume <100 µl) in polystyrene round-bottom tubes. Lentiviruses were added at 20 Plaque Forming Units per cell (PFU/cell), assuming 1000 cells/islet. The final volume did not exceed 300 µl and virus concentration used was 1.7 x 10^4 PFU/µl. 5 µg/ml of polybrene was added for infection. Islets were incubated overnight in a cell culture incubator and then transplanted or incubated in 12-well suspension plates (37ºC, 5% CO_2) to assess knockdown efficiency and VEGF-A secretion.

Statistical analysis.

GraphPad Prism (Prism version 6.00 for Windows, GraphPad Software, La Jolla California USA, www.graphpad.com) was used for analysis. Data are depicted as mean ± SEM unless otherwise specified. An unpaired Student's *t*-test was performed to analyze variances between two populations. Two-way ANOVA (Bonferroni's post hoc test) was used to compare multiple populations.

Supplementary Materials

References and Notes:

1. A. Bruni, B. Gala-Lopez, A. R. Pepper, N. S. Abualhassan, A. J. Shapiro, Islet cell transplantation for the treatment of type 1 diabetes: recent advances and future challenges., *Diabetes. Metab. Syndr. Obes.* **7**, 211–23 (2014).

2. G. Mattsson, L. Jansson, P.-O. Carlsson, Decreased vascular density in mouse pancreatic islets after transplantation., *Diabetes* **51**, 1362–6 (2002).

3. P.-O. Carlsson, F. Palm, G. Mattsson, Low revascularization of experimentally transplanted human pancreatic islets., *J. Clin. Endocrinol. Metab.* **87**, 5418–23 (2002).

4. M. Brissova, A. C. Powers, Revascularization of transplanted islets: can it be improved?, *Diabetes* **57**, 2269–71 (2008).

5. L. Jansson, P.-O. P.-O. Carlsson, Graft vascular function after transplantation of pancreatic islets, *Diabetologia* **45**, 749–763 (2002).

6. N. Ballian, F. C. Brunicardi, Islet vasculature as a regulator of endocrine pancreas function., *World J. Surg.* **31**, 705–14 (2007).

7. A. M. Davalli, L. Scaglia, D. H. Zangen, J. Hollister, S. Bonner-Weir, G. C. Weir, Vulnerability of islets in the immediate posttransplantation period. Dynamic changes in structure and function., *Diabetes* **45**, 1161–7 (1996).

8. M. D. Menger, J. Yamauchi, B. Vollmar, Revascularization and microcirculation of freely grafted islets of Langerhans., *World J. Surg.* **25**, 509–15 (2001).

9. P. Vajkoczy, M. D. Menger, E. Simpson, K. Messmer, Angiogenesis and vascularization of murine pancreatic islet isografts., *Transplantation* **60**, 123–7 (1995).

10. P.-O. O. Carlsson, F. Palm, A. Andersson, P. Liss, Markedly decreased oxygen tension in transplanted rat pancreatic islets irrespective of the implantation site., *Diabetes* **50**, 489–95 (2001).

11. B. Vasir, J. C. Jonas, G. M. Steil, J. Hollister-Lock, W. Hasenkamp, A. Sharma, S. Bonner-Weir, G. C. Weir, Gene expression of VEGF and its receptors Flk-1/KDR and Flt-1 in cultured and transplanted rat islets., *Transplantation* **71**, 924–35 (2001).

12. M. Brissova, M. Fowler, P. Wiebe, A. Shostak, M. Shiota, A. Radhika, P. C. Lin, M. Gannon, A. C. Powers, Intraislet endothelial cells contribute to revascularization of transplanted pancreatic islets., *Diabetes* **53**, 1318–25 (2004).

13. T. Linn, K. Schneider, H. P. Hammes, K. T. Preissner, H. Brandhorst, E. Morgenstern, F. Kiefer, R. G. Bretzel, Angiogenic capacity of endothelial cells in islets of Langerhans., *FASEB J.* **17**, 881–3 (2003).

14. D. Nyqvist, M. Köhler, H. Wahlstedt, P.-O. Berggren, Donor islet endothelial cells participate in formation of functional vessels within pancreatic islet grafts., *Diabetes* **54**, 2287–93 (2005).

15. G. D. Yancopoulos, S. Davis, N. W. Gale, J. S. Rudge, S. J. Wiegand, J. Holash, Vascular-specific growth factors and blood vessel formation., *Nature* **407**, 242–8 (2000).

16. M. Brissova, A. Shostak, M. Shiota, P. O. Wiebe, G. Poffenberger, J. Kantz, Z. Chen, C. Carr, W. G. Jerome, J. Chen, H. S. Baldwin, W. Nicholson, D. M. Bader, T. Jetton, M. Gannon, A. C. Powers, Pancreatic Islet Production of Vascular Endothelial Growth Factor-A Is Essential for Islet Vascularization, Revascularization, and Function, *Diabetes* **55**, 2974–2985 (2006).

17. Q. Cai, M. Brissova, R. B. Reinert, F. Cheng Pan, P. Brahmachary, M. Jeansson, A. Shostak, A. Radhika, G. Poffenberger, S. E. Quaggin, W. Gray Jerome, D. J. Dumont, A. C. Powers, F. C. Pan, P. Brahmachary, M. Jeansson, A. Shostak, A. Radhika, G. Poffenberger, S. E. Quaggin, W. G. Jerome, D. J. Dumont, A. C. Powers, Enhanced expression of VEGF-A in β cells increases endothelial cell number but impairs islet morphogenesis and β cell proliferation., *Dev. Biol.* **367**, 40–54 (2012).

18. M. Brissova, K. Aamodt, P. Brahmachary, N. Prasad, J. Y. Hong, C. Dai, M. Mellati, A. Shostak, G. Poffenberger, R. Aramandla, S. E. Levy, A. C. Powers, Islet Microenvironment, Modulated by Vascular Endothelial Growth Factor-A Signaling, Promotes beta Cell Regeneration, *Cell Metab* (2014).

19. J. Agudo, E. Ayuso, V. Jimenez, A. Casellas, C. Mallol, A. Salavert, S. Tafuro, M. Obach, A. Ruzo, M. Moya, A. Pujol, F. Bosch, Vascular endothelial growth factor-mediated islet hypervascularization and inflammation contribute to progressive reduction of β-cell mass., *Diabetes* **61**, 2851–61 (2012).

20. P. Büchler, H. A. Reber, M. M. W. Büchler, S. Shrinkante, M. M. W. Büchler, H. Friess, G. L. Semenza, O. J. Hines, Hypoxia-inducible factor 1 regulates vascular endothelial growth factor expression in human pancreatic cancer., *Pancreas* **26**, 56–64 (2003).

21. D. L. Gorden, S. J. Mandriota, R. Montesano, L. Orci, M. S. Pepper, Vascular endothelial growth factor is increased in devascularized rat islets of Langerhans in vitro., *Transplantation* **63**, 436–43 (1997).

22. Z. Arany, S.-Y. Foo, Y. Ma, J. L. Ruas, A. Bommi-Reddy, G. Girnun, M. Cooper, D. Laznik, J. Chinsomboon, S. M. Rangwala, K. H. Baek, A. Rosenzweig, B. M. Spiegelman, HIF-independent regulation of VEGF and angiogenesis by the transcriptional coactivator PGC-1alpha., *Nature* **451**, 1008–12 (2008).

23. P. J. Willy, I. R. Murray, J. Qian, B. B. Busch, W. C. Stevens, R. Martin, R. Mohan, S. Zhou,

P. Ordentlich, P. Wei, D. W. Sapp, R. A. Horlick, R. A. Heyman, I. G. Schulman, Regulation of PPARgamma coactivator 1alpha (PGC-1alpha) signaling by an estrogen-related receptor alpha (ERRalpha) ligand., *Proc. Natl. Acad. Sci. U. S. A.* **101**, 8912–7 (2004).

24. S. N. Schreiber, D. Knutti, K. Brogli, T. Uhlmann, A. Kralli, The Transcriptional Coactivator PGC-1 Regulates the Expression and Activity of the Orphan Nuclear Receptor Estrogen-Related Receptor α (ERRα), *J. Biol. Chem.* **278**, 9013–9018 (2003).

25. N. K. Tonks, Protein tyrosine phosphatases: from genes, to function, to disease., *Nat. Rev. Mol. Cell Biol.* **7**, 833–46 (2006).

26. Y. Wallez, I. Vilgrain, P. Huber, Angiogenesis: the VE-cadherin switch., *Trends Cardiovasc. Med.* **16**, 55–9 (2006).

27. Y. Nakamura, N. Patrushev, H. Inomata, D. Mehta, N. Urao, H. W. Kim, M. Razvi, V. Kini, K. Mahadev, B. J. Goldstein, R. McKinney, T. Fukai, M. Ushio-Fukai, Role of Protein Tyrosine Phosphatase 1B in Vascular Endothelial Growth Factor Signaling and Cell-Cell Adhesions in Endothelial Cells, *Circ. Res.* **102**, 1182–1191 (2008).

28. Y. Chang, Increase of PTP levels in vascular injury and in cultured aortic smooth muscle cells treated with specific growth factors, *AJP Hear. Circ. Physiol.* **287**, H2201–H2208 (2004).

29. Á. González-Rodriguez, Ó. Escribano, J. Alba, C. M. Rondinone, M. Benito, Á. M. Valverde, A. González-Rodriguez, O. Escribano, J. Alba, C. M. Rondinone, M. Benito, A. M. Valverde, Á. González-Rodriguez, Ó. Escribano, J. Alba, C. M. Rondinone, M. Benito, Á. M. Valverde, Levels of protein tyrosine phosphatase 1B determine susceptibility to apoptosis in serum-deprived hepatocytes., *J. Cell. Physiol.* **212**, 76–88 (2007).

30. A. Bettaieb, S. Liu, Y. Xi, N. Nagata, K. Matsuo, I. Matsuo, S. Chahed, J. Bakke, H. Keilhack, T. Tiganis, F. G. Haj, Differential Regulation of Endoplasmic Reticulum Stress by Protein Tyrosine Phosphatase 1B and T Cell Protein Tyrosine Phosphatase, *J. Biol. Chem.* **286**, 9225–9235 (2011).

31. R. Fernandez-Ruiz, E. Vieira, P. M. Garcia-Roves, R. Gomis, Protein tyrosine phosphatase-1B modulates pancreatic β-cell mass., *PLoS One* **9**, e90344 (2014).

32. S. Speier, D. Nyqvist, O. Cabrera, J. Yu, R. D. Molano, A. Pileggi, T. Moede, M. Köhler, J. Wilbertz, B. Leibiger, C. Ricordi, I. B. Leibiger, A. Caicedo, P.-O. Berggren, Noninvasive in

vivo imaging of pancreatic islet cell biology, *Nat. Med.* **14**, 574–578 (2008).

33. S. Speier, D. Nyqvist, M. Köhler, A. Caicedo, I. B. Leibiger, P.-O. Berggren, Noninvasive high-resolution in vivo imaging of cell biology in the anterior chamber of the mouse eye., *Nat. Protoc.* **3**, 1278–86 (2008).

34. E. Adeghate, Host-graft circulation and vascular morphology in pancreatic tissue transplants in rats., *Anat. Rec.* **251**, 448–59 (1998).

35. E. Adeghate, T. Donáth, Morphological findings in long-term pancreatic tissue transplants in the anterior eye chamber of rats., *Pancreas* **5**, 298–305 (1990).

36. S. W. Cousins, M. M. McCabe, D. Danielpour, J. W. Streilein, Identification of transforming growth factor-beta as an immunosuppressive factor in aqueous humor., *Invest. Ophthalmol. Vis. Sci.* **32**, 2201–11 (1991).

37. J. Y. Niederkorn, Immune privilege in the anterior chamber of the eye., *Crit. Rev. Immunol.* **22**, 13–46 (2002).

38. M. D. Menger, S. Jaeger, P. Walter, G. Feifel, F. Hammersen, K. Messmer, Angiogenesis and hemodynamics of microvasculature of transplanted islets of Langerhans., *Diabetes* **38 Suppl 1**, 199–201 (1989).

39. A. Del Toro-Arreola, A. K. Robles-Murillo, A. Daneri-Navarro, J. D. Rivas-Carrillo, The role of endothelial cells on islet function and revascularization after islet transplantation, *Organogenesis* **12**, 28–32 (2016).

40. N. Fotino, C. Fotino, A. Pileggi, Re-engineering islet cell transplantation., *Pharmacol. Res.* **98**, 76–85 (2015).

41. D. Nyqvist, S. Speier, R. Rodriguez-Diaz, R. D. Molano, S. Lipovsek, M. Rupnik, A. Dicker, E. Ilegems, E. Zahr-Akrawi, J. Molina, M. Lopez-Cabeza, S. Villate, M. H. Abdulreda, C. Ricordi, A. Caicedo, A. Pileggi, P.-O. Berggren, Donor Islet Endothelial Cells in Pancreatic Islet Revascularization, *Diabetes* **60**, 2571–2577 (2011).

42. H. Liljebäck, L. Grapensparr, J. Olerud, P.-O. Carlsson, Extensive Loss of Islet Mass beyond the First Day after Intraportal Human Islet Transplantation in a Mouse Model, *Cell Transplant.* **25**, 481–489 (2016).

43. P. Lopez, K.-D. Wagner, P. Hofman, E. Van Obberghen, RNA Activation of the Vascular Endothelial Growth Factor Gene (VEGF) Promoter by Double-Stranded RNA and Hypoxia: Role of Noncoding VEGF Promoter Transcripts., *Mol. Cell. Biol.* **36**, 1480–93 (2016).

44. A. Boker, L. Rothenberg, C. Hernandez, N. S. Kenyon, C. Ricordi, R. Alejandro, Human islet transplantation: update., *World J. Surg.* **25**, 481–6 (2001).

45. M. D. Mueller, J. L. Vigne, A. Minchenko, D. I. Lebovic, D. C. Leitman, R. N. Taylor, Regulation of vascular endothelial growth factor (VEGF) gene transcription by estrogen receptors alpha and beta., *Proc. Natl. Acad. Sci. U. S. A.* **97**, 10972–7 (2000).

46. G. Pagès, J. Pouysségur, Transcriptional regulation of the Vascular Endothelial Growth Factor gene--a concert of activating factors., *Cardiovasc. Res.* **65**, 564–73 (2005).

47. M. McCall, A. M. J. Shapiro, Update on islet transplantation., *Cold Spring Harb. Perspect. Med.* **2**, a007823 (2012).

48. G. L. Warnock, Y. H. T. Liao, X. Wang, D. Ou, Z. Ao, J. D. Johnson, C. B. Verchere, D. Thompson, An odyssey of islet transplantation for therapy of type 1 diabetes., *World J. Surg.* **31**, 1569–76 (2007).

49. A. R. Pepper, B. Gala-Lopez, O. Ziff, A. M. J. Shapiro, Revascularization of transplanted pancreatic islets and role of the transplantation site., *Clin. Dev. Immunol.* **2013**, 352315 (2013).

50. M. Goel, R. G. Picciani, R. K. Lee, S. K. Bhattacharya, Aqueous humor dynamics: a review., *Open Ophthalmol. J.* **4**, 52–9 (2010).

51. M. Aihara, J. D. Lindsey, R. N. Weinreb, Aqueous humor dynamics in mice., *Invest. Ophthalmol. Vis. Sci.* **44**, 5168–73 (2003).

52. A. Haddad, E. M. Laicine, J. C. de Almeida, Origin and renewal of the intrinsic glycoproteins of the aqueous humor., *Graefe's Arch. Clin. Exp. Ophthalmol. = Albr. von Graefes Arch. für Klin. und Exp. Ophthalmol.* **229**, 371–9 (1991).

53. L. D. Klaman, O. Boss, O. D. Peroni, J. K. Kim, J. L. Martino, J. M. Zabolotny, N. Moghal, M. Lubkin, Y. B. Kim, A. H. Sharpe, A. Stricker-Krongrad, G. I. Shulman, B. G. Neel, B. B. Kahn, Increased energy expenditure, decreased adiposity, and tissue-specific insulin sensitivity in protein-tyrosine phosphatase 1B-deficient mice., *Mol. Cell. Biol.* **20**, 5479–89 (2000).

54. K. Hayashi, R. Kojima, M. Ito, Strain differences in the diabetogenic activity of streptozotocin in mice., *Biol. Pharm. Bull.* **29**, 1110–9 (2006).

55. M. C. Deeds, J. M. Anderson, A. S. Armstrong, D. A. Gastineau, H. J. Hiddinga, A. Jahangir, N. L. Eberhardt, Y. C. Kudva, Single dose streptozotocin-induced diabetes: considerations for study design in islet transplantation models., *Lab. Anim.* **45**, 131–40 (2011).

56. I. E. Dumitriu, W. Mohr, W. Kolowos, P. Kern, J. R. Kalden, M. Herrmann, 5,6-Carboxyfluorescein Diacetate Succinimidyl Ester-Labeled Apoptotic and Necrotic as Well as Detergent-Treated Cells Can Be Traced in Composite Cell Samples, *Anal. Biochem.* **299**, 247–252 (2001).

57. T. C. Brelje, D. W. Scharp, R. L. Sorenson, Three-dimensional imaging of intact isolated islets of Langerhans with confocal microscopy., *Diabetes* **38**, 808–14 (1989).

58. A. L. C. Figueroa, H. Figueiredo, S. A. Rebuffat, E. Vieira, R. Gomis, Taurine Treatment Modulates Circadian Rhythms in Mice Fed A High Fat Diet, **6**, 36801 (2016).

59. J. Altirriba, R. Gasa, S. Casas, M. J. Ramírez-Bajo, S. Ros, A. Gutierrez-Dalmau, M. C. Ruiz de Villa, A. Barbera, R. Gomis, The role of transmembrane protein 27 (TMEM27) in islet physiology and its potential use as a beta cell mass biomarker, *Diabetologia* **53**, 1406–1414 (2010).

60. C. Broca, E. Varin, M. Armanet, C. Tourrel-Cuzin, D. Bosco, S. Dalle, A. Wojtusciszyn, Proteasome dysfunction mediates high glucose-induced apoptosis in rodent beta cells and human islets., *PLoS One* **9**, e92066 (2014).

61. C. M. Jimenez-Moreno, I. de G. Herrera-Gomez, L. Lopez-Noriega, P. I. Lorenzo, N. Cobo-Vuilleumier, E. Fuente-Martin, J. M. Mellado-Gil, G. Parnaud, D. Bosco, B. R. Gauthier, A. Martin-Montalvo, A Simple High Efficiency Intra-Islet Transduction Protocol Using Lentiviral Vectors., *Curr. Gene Ther.* **15**, 436–46 (2015).

62. F. Li, R. I. Mahato, RNA interference for improving the outcome of islet transplantation., *Adv. Drug Deliv. Rev.* **63**, 47–68 (2011).

63. J.-R. Bertrand, M. Pottier, A. Vekris, P. Opolon, A. Maksimenko, C. Malvy, Comparison of antisense oligonucleotides and siRNAs in cell culture and in vivo., *Biochem. Biophys. Res. Commun.* **296**, 1000–4 (2002).

64. T. B. Murdoch, D. McGhee-Wilson, A. M. J. Shapiro, J. R. T. Lakey, Methods of Human Islet Culture for Transplantation, *Cell Transplant.* **13**, 605–617 (2004).

65. A. Pollack, G. Ciancio, Cell cycle phase-specific analysis of cell viability using Hoechst 33342 and propidium iodide after ethanol preservation., *Methods Cell Biol.* **33**, 19–24 (1990).

Acknowledgements: We thank Y. Esteban (Institut d'Investigacions Biomèdiques August Pi i Sunyer, IDIBAPS/Centro de Investigación Biomédica en Red de Diabetes y Enfermedades Metabólicas Asociadas, CIBERDEM, Barcelona, Spain) for excellent technical support in immunoblotting analysis. We thank K. Katte (IDIBAPS/CIBERDEM, Barcelona, Spain) and B. Sinclair for English proofreading the manuscript. We are grateful to all members of the Gomis-Gasa group for plentiful and rich discussions.

Funding: This work has been supported by projects PI13/01500 and PI16/00774 (to R. Gasa and R. Gomis) integrated in the Plan Estatal de I+D+I and cofinanced by ISCIII-Subdirección General de Evaluación and Fondo Europeo de Desarrollo Regional (FEDER-"A way to build Europe"); grant 2014 SGR659 (to R. Gomis) from the Generalitat de Catalunya; Recerca Bàsica grant (to R. Gomis) from the Academy of Medical and Health Science of Catalonia and the Balearic Islands; and Cátedra Astra Zeneca. H.F was partly supported by DiabetesCero Foundation grant. A.L.C.F. was supported by a Doctoral fellowship from the Consejo Nacional de Ciencia y Tecnologia (CONACYT) from México.

Author contributions: H.F. conducted all experiments. A.L.C.F. performed and provided assistance with mouse and human islets experiments. A.G. and R.M. provide assistance with mouse experiments and immunohistochemistry studies in paraffinized eye sections. C.B. and A.W. performed isolation of human islets and provide assistance with human islet experiments.

R.M. and R.F.R. performed experiments. H.F., R.M., and R.Gomis conceived the project. H.F., R.M., R.Gasa, and R.Gomis discussed the data. H.F., R.Gasa, and R.Gomis wrote the manuscript. R.Gasa and R.Gomis are corresponding authors.

Competing interests: There is NO Competing Interest.

Data and materials availability: All data needed to evaluate the conclusions in the paper are present in the paper and/or the Supplementary Materials.

Figure legends

Fig. 1. PTP1B$^{-/-}$ mouse islets present reduced endothelial cell loss in vitro. Pancreatic islets from adult PTP1B$^{+/+}$ and PTP1B$^{-/-}$ mice were cultured for two days and processed for immunofluorescence and gene expression analysis. (**A)** Representative maximum projections of image stacks and (**B**) quantification of percentage of PECAM-1^{+} area relative to total islet area in freshly-isolated and two-day cultured PTP1B$^{+/+}$ (550 cells x 15 islets) and PTP1B$^{-/-}$ (500 cells x 15 islets) islets; scale bars, 25µm. (**C**) qRT-PCR of the vascular marker genes *Pecam1, Kdr,* and *Cdh5* in two-day cultured PTP1B$^{+/+}$ (n = 9) and PTP1B$^{-/-}$ (n = 12) islets. (**D)** Representative images of in toto immunofluorescence staining of cleaved-CASPASE3 (green) and INSULIN (pink) in two-day cultured PTP1B$^{+/+}$ and PTP1B$^{-/-}$ islets. Nuclei (blue) were stained using Hoechst; scale bars, 25 µm. (**E**) Quantification of cleaved CASPASE-3^{+} cells relative to total islet cells in PTP1B$^{+/+}$ (n = 550 cells x 15 islets) and PTP1B$^{-/-}$ (n = 550 cells x 15 islets) islets. (**F**) qRT-PCR of the apoptotic genes *Casp3* and *Casp9* in PTP1B$^{+/+}$ (n = 9) and PTP1B$^{-/-}$ (n = 12) islets. Data presented are mean ± SEM. n.s. (not significant), $^{**}P < 0.01$, by one-way ANOVA for (B); $^{*}P < 0.05$, $^{**}P < 0.01$, n.s. by Student's t-test for (C,E,F).

Fig. 2. Transplanted PTP1B$^{-/-}$ mouse islets restore normoglycemia and circulating insulin concentration in diabetic mice. (**A**) Schematic diagram and representative image of islets transplanted into the anterior chamber of a mouse eye; scale bar, 2 mm. **(B-G)** BALB/c mice were divided into 4 experimental groups: non-diabetic mice (n = 8) and STZ-induced diabetic mice transplanted with PTP1B$^{+/+}$ islets (PTP1B$^{+/+}$tx$^{balb\text{-}stz}$, n = 10), PTP1B$^{-/-}$ islets (PTP1B$^{-/-}$tx$^{balb\text{-}stz}$, n = 12) or non-transplanted (n = 10). (**B**) Blood glucose concentration measured at the indicated times. Median blood glucose concentration at day 0 (transplantation) is 340 mg/dL and is represented as a dashed line. Normoglycemia (120 mg/dL) is set as the average blood glucose of non-diabetic mice during the 28-day follow up period and is also represented as a dashed line. (**C**) Body weight measured at the indicated times. (**D**) Intraperitoneal glucose tolerance test (IPGTT) performed at day 28 post-transplant (n=5). (**E**) Calculation of the area under curve of the IPGTT. (**F**) Plasma insulin concentration during the IPGTT (n=5). (**G**) Pancreatic insulin content at day 28 post-transplant, expressed relative to non-diabetic mice (normalized as 1, n=6). Data are presented as mean ± SEM. *$P < 0.05$, **$P < 0.01$ for PTP1B$^{+/+}$tx$^{balb\text{-}stz}$ vs PTP1B$^{-/-}$tx$^{balb\text{-}stz}$, #$P < 0.05$ for PTP1B$^{+/+}$tx$^{balb\text{-}stz}$ vs non-transplanted, n.s. for PTP1B$^{-/-}$tx$^{balb\text{-}stz}$ vs not diabetic mice, \$\$\$$P < 0.001$ for non-diabetic vs PTP1B$^{-/-}$tx$^{balb\text{-}stz}$, by two-way ANOVA; ***$P < 0.001$, by one-way ANOVA in (G).

Fig. 3. PTP1B$^{-/-}$ mouse islet grafts exhibit improved revascularization and survival without loss of ß-cell area. (**A**) Representative in vivo images of functional vessels (RITC-dextran, red) and cell death (PI, white) in PTP1B$^{+/+}$tx$^{balb\text{-}stz}$ and PTP1B$^{-/-}$tx$^{balb\text{-}stz}$ eye grafts at 7, 15, and 28 days following transplant (Tx); nuclei are labeled with Hoechst (blue); CFDA-stained islet cells (green); scale bars, 25 µm. (**B**) Relative vascular density at the indicated times. (**C**) Percentage of

vascularization area relative to total islet area at the indicated times. (**D**) Percentage of PI^+ cells at day 28 post-Tx (600 cells x 8 islets/animal) in $PTP1B^{+/+}tx^{balb\text{-}stz}$ and $PTP1B^{-/-}tx^{balb\text{-}stz}$ grafts (*n* = 8 islets x 10 animals). (**E**) Representative immunofluorescence images for cleaved CASPASE-3 (green), glucagon (pink) and insulin (pink, green) in eye sections from $PTP1B^{+/+}tx^{balb\text{-}stz}$ and $PTP1B^{-/-}tx^{balb\text{-}stz}$ animals collected at day 28 post-Tx; scale bars, 25 μm. (**F**) Percentage of cleaved CASPASE-3^+ cells relative to $INSULIN^+$ cells in $PTP1B^{+/+}tx^{balb\text{-}stz}$ and $PTP1B^{-/-}tx^{balb\text{-}stz}$ grafts (*n* = 10 islets x 6 animals) grafts. (**G**) Percentage of $INSULIN^+$ area relative to total graft area in $PTP1B^{+/+}tx^{balb\text{-}stz}$ and $PTP1B^{-/-}tx^{balb\text{-}stz}$ grafts (*n* = 5 islets x 6 animals). Data presented as mean ± SEM. **P* < 0.05, ***P* < 0.01, by two-way ANOVA in (B,C); **P* < 0.05, ***P* < 0.01, ****P* < 0.001, by Student's t-test in (D,F,G).

Fig. 4. IECs are not responsible for improved revascularization of $PTP1B^{-/-}$ mouse islet grafts. (**A**) Representative maximum projections of image stacks of PECAM-1 immunofluorescence staining (yellow) in $PTP1B^{+/+}$ and $PTP1B^{-/-}$ mouse islets cultured for 0, 2, and 7 days; a white line defines islet area; scale bars 25 μm. (**B**) Relative PECAM-1^+ area in relation to total islet area (*n* = 600 cells x 9 islets). (**C, D**) Blood glucose concentration and body weight of $PTP1B^{+/+}EC^{\varnothing}tx^{balb\text{-}stz}$ (*n* = 7) and $PTP1B^{-/-}$ $EC^{\varnothing}tx^{balb\text{-}stz}$ (*n* = 7) mice at the indicated times; median concentration of blood glucose at day 0: 347 mg/dL; average concentration of blood glucose of non-diabetic mice: 120 mg/dL (*n* = 8); diabetes threshold: 250 mg/dL. (**E**) Representative immunofluorescence images of PECAM-1 (green), cleaved CASPASE-3 (green), and INSULIN (pink) in grafts 28 days post-tx; nuclei are labeled with Hoechst (blue). (**F,G**) Quantification of PECAM-1^+ area relative to $INSULIN^+$ area and cleaved CASPASE-3^+ cells relative to $INSULIN^+$ cells in $PTP1B^{+/+}EC^{\varnothing}tx^{balb\text{-}stz}$ and $PTP1B^{-/-}EC^{\varnothing}tx^{balb\text{-}stz}$ grafts; scale bars, 25

μm; *n* = 550 cells x 7 islets/animal, 5 animals. Data presented as mean ± SEM. n.s. not significant, **P* < 0.05, ***P* < 0.01, by one-way ANOVA in (C,D); **P* < 0.05, ***P* < 0.01, n.s. by Student's t-test in (B,F,G).

Fig. 5. PTP1B$^{-/-}$ mouse islets exhibit enhanced VEGF-A production and activation of the PGC1α/ERRα axis (**A**) Representative immunofluorescence images of VEGF-A (yellow) and INSULIN (pink) staining in PTP1B$^{+/+}$tx$^{balb\text{-}stz}$ and PTP1B$^{-/-}$tx$^{balb\text{-}stz}$ grafts 28 days after transplantation; nuclei are labeled with Hoechst (blue); scale bars, 25 μm. (**B**) Quantification of VEGF-A^{+}/INSULIN^{+} cells relative to total INSULIN^{+} cells in PTP1B$^{+/+}$tx$^{balb\text{-}stz}$ (*n* = 8 islets/animal x 9 animals) and PTP1B$^{-/-}$tx$^{balb\text{-}stz}$ (*n* = 10 islets x 7 animals) grafts. (**C**) *Vegfa* expression in two-day cultured PTP1B$^{+/+}$ and PTP1B$^{-/-}$ islets determined by qRT-PCR and expressed relative to PTP1B$^{+/+}$ (normalized as 1) (*n* = 9). (**D**) Representative immunofluorescence images of INSULIN (pink) and VEGF-A (green) in two-day cultured PTP1B$^{+/+}$ and PTP1B$^{-/-}$ islets; nuclei are labeled with Hoechst (blue). (**E**) Quantification of VEGF-A^{+}/INSULIN^{+} cells relative to total INSULIN^{+} cells in two-day cultured PTP1B$^{+/+}$ and PTP1B$^{-/-}$ islets; scale bars: 25 μm; (*n* = 700 cells x 14 islets). (**F**) VEGF-A secretion (normalized by content) from two-day cultured PTP1B$^{+/+}$ and PTP1B$^{-/-}$ islets (*n* = 6) determined by ELISA. (**G**) qRT-PCR of *Hif1a, Ppargc1a,* and *Esrra* in two-day cultured PTP1B$^{+/+}$ and PTP1B$^{-/-}$ islets (*n* = 9). (**H**) Representative immunoblot for PGC1α (105 kDa) and αTUBULIN (52 kDa) in whole cell extracts, and for HIF1α (120 kDa), ERRα (52 kDa) and LAMIN-B (66 kDa) in nuclear extracts of PTP1B$^{+/+}$ and PTP1B$^{-/-}$ islets cultured for 2 days in complete medium or Hbss (*n* = 2). (**I**, **J**) qRT-PCR of *Vegfa, Ppargc1a,* and *Esrra* in PTP1B$^{+/+}$ **(I)** and PTP1B$^{-/-}$ (**J**) islets cultured in complete medium or Hbss (*n* = 10). (**K**) qRT-PCR of *Hif1a, Vegfa, Ppargc1a,* and

Esrra in PTP1B$^{+/+}$ and PTP1B$^{-/-}$ islets cultured in Hbss (n = 10). (**L**) VEGF-A secretion (normalized by total protein content) from PTP1B$^{+/+}$ and PTP1B$^{-/-}$ islets cultured in complete medium or Hbss (n = 6). Data presented as mean ± SEM. n.s., not significant, *P < 0.05, **P < 0.01, ***P < 0.001, by Student's t-test in (B, C, E, F, G, I, J, K) and by two-way ANOVA in (L).

Fig. 6. PTP1B silencing in human islets induces VEGF-A expression and improves graft vascularization (**A**) Immunoblot for PTP1B and αTUBULIN using whole cell extracts from scrambled-siRNA and PTP1B-siRNA-treated islets 3 days after transfection. (**B**) Representative immunofluorescence images of INSULIN (green) and PTP1B (pink) in scrambled-siRNA and PTP1B-siRNA-treated islets 3 days after transfection; nuclei are labeled with Hoechst (blue) (n = 8). (**C**) Percentage of PTP1B^{+}/INSULIN^{+} cells relative to total INSULIN^{+} cells in PTP1B-siRNA and scrambled-siRNA-transfected human islets (n = 8 islets x 700 cells/islet). (**D**) qRT-PCR for *PTPN1*, *HIF1A*, *VEGFA*, *PPARGC1A,* and *ESRRA* in scrambled-siRNA (n = 6) and PTP1B-siRNA-treated islets (n = 6) 3 days after transfection. qRT-PCR for *GAPDH* in human islets transfected with *GAPDH*-siRNA or left untransfected (control) is shown as positive control. (**E**) Secretion of VEGF-A (normalized by total protein content) from scrambled-siRNA and PTPB1-siRNA-treated islets (n = 4). (**F**) Fluorescence images of islets infected with shPTPN1 LV (encoding GFP) and non-infected (control) islets 2 and 8 days after lentiviral infection; scale bars 50 μm. Insets shown at higher magnification. (**G**) Immunoblot for PTP1B and αTUBULIN in cell extracts of human islets 2 and 8 days after infection with sh-scrambled LV or sh-PTP1B LV. (**H**) Secretion of VEGF-A (normalized by total protein content) from human islets 2 and 8 days after infection with sh-scrambled LV or sh-PTP1B LV (n = 4). (**I**) Representative in vivo

intraocular images of functional vessels using RITC-dextran (red) in sh-scrambled LV and sh-PTP1B LV islet grafts 8 days after transplantation; GFP fluorescence (green) shows human islet cells infected with sh-scrambled LV and sh-PTP1B LV; scale bars, 25 μm. Data presented as mean ± SEM. *$P < 0.05$, **$P < 0.01$ by Student's t-test in (C, D, E) and by two-way ANOVA in (H).

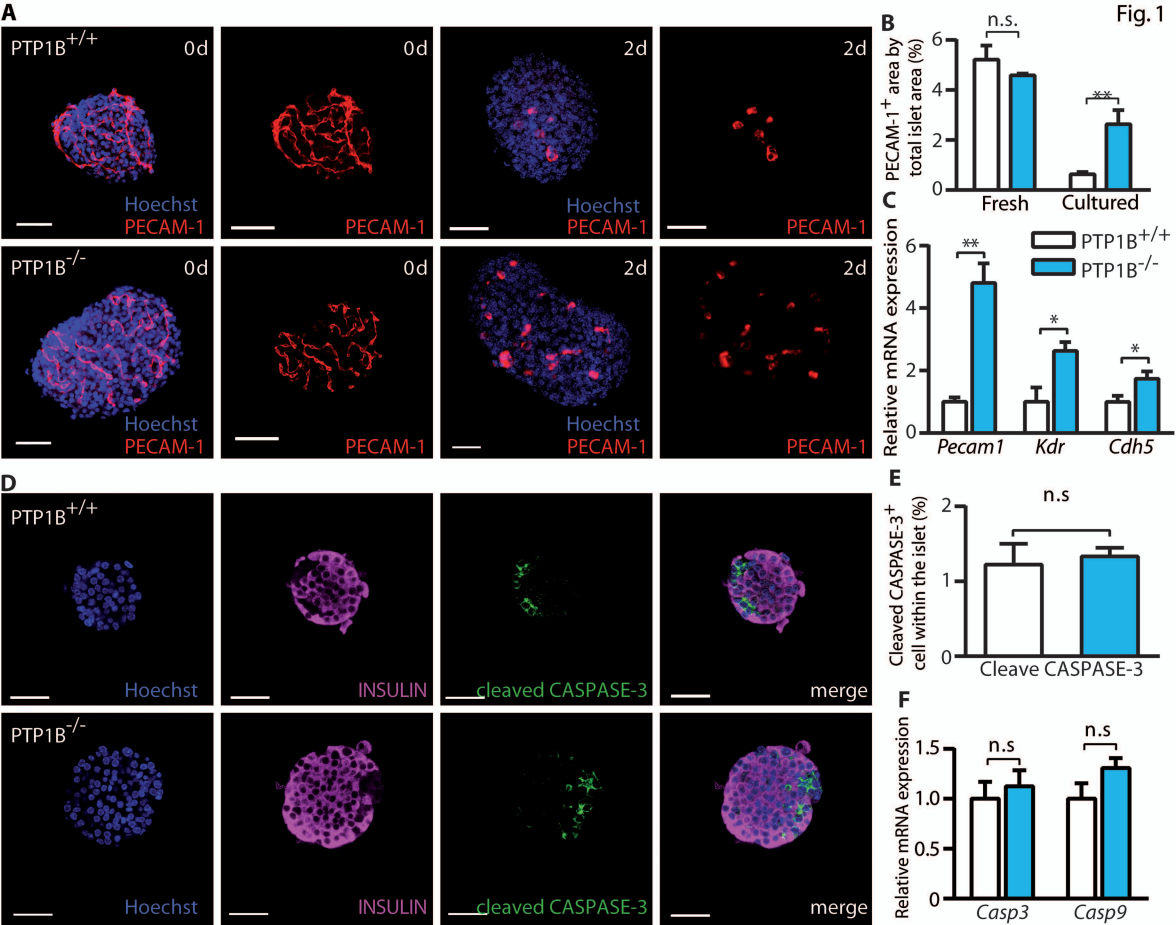
Fig.1
A
PTP1B+/+
0d
0d
2d
2d
Hoechst
PECAM-1
PTP1B-/-
B
n.s.
**
PECAM-1+ area by total islet area (%)
Fresh
Cultured
C
PTP1B+/+
PTP1B-/-
Relative mRNA expression
**
*
*
Pecam1
Kdr
Cdh5
D
Hoechst
INSULIN
cleaved CASPASE-3
merge
E
n.s
Cleaved CASPASE-3+ cell within the islet (%)
Cleave CASPASE-3
F
n.s
n.s
Relative mRNA expression
Casp3
Casp9

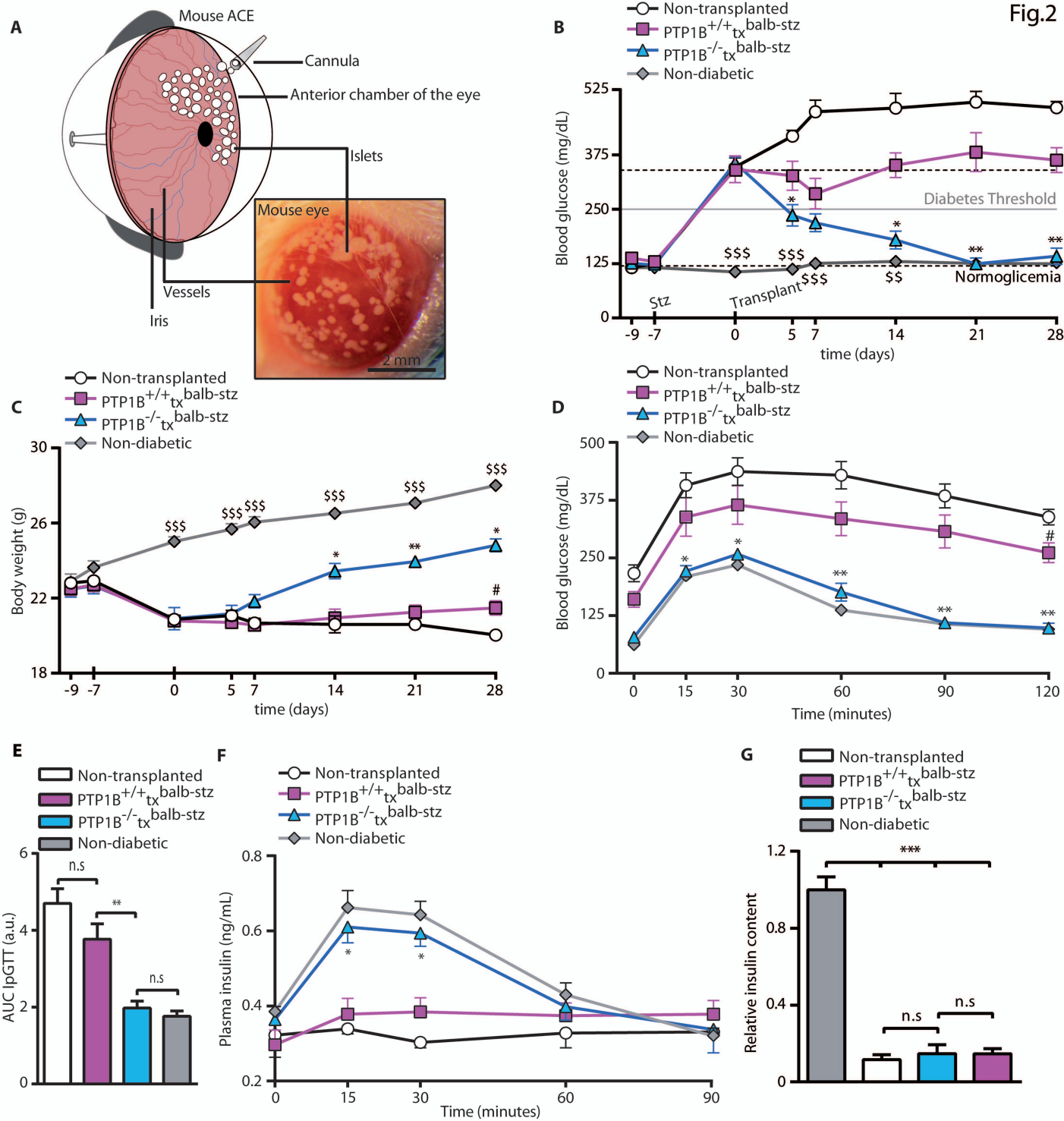
Fig.2
A
Mouse ACE
Cannula
Anterior chamber of the eye
Islets
Mouse eye
Vessels
Iris
2 mm
B
Non-transplanted
PTP1B+/+tx balb-stz
PTP1B-/-tx balb-stz
Non-diabetic
Blood glucose (mg/dL)
Diabetes Threshold
Normoglicemia
Stz
Transplant
time (days)
C
Body weight (g)
time (days)
D
Blood glucose (mg/dL)
Time (minutes)
E
AUC IpGTT (a.u.)
n.s
F
Plasma insulin (ng/mL)
Time (minutes)
G
Relative insulin content
n.s

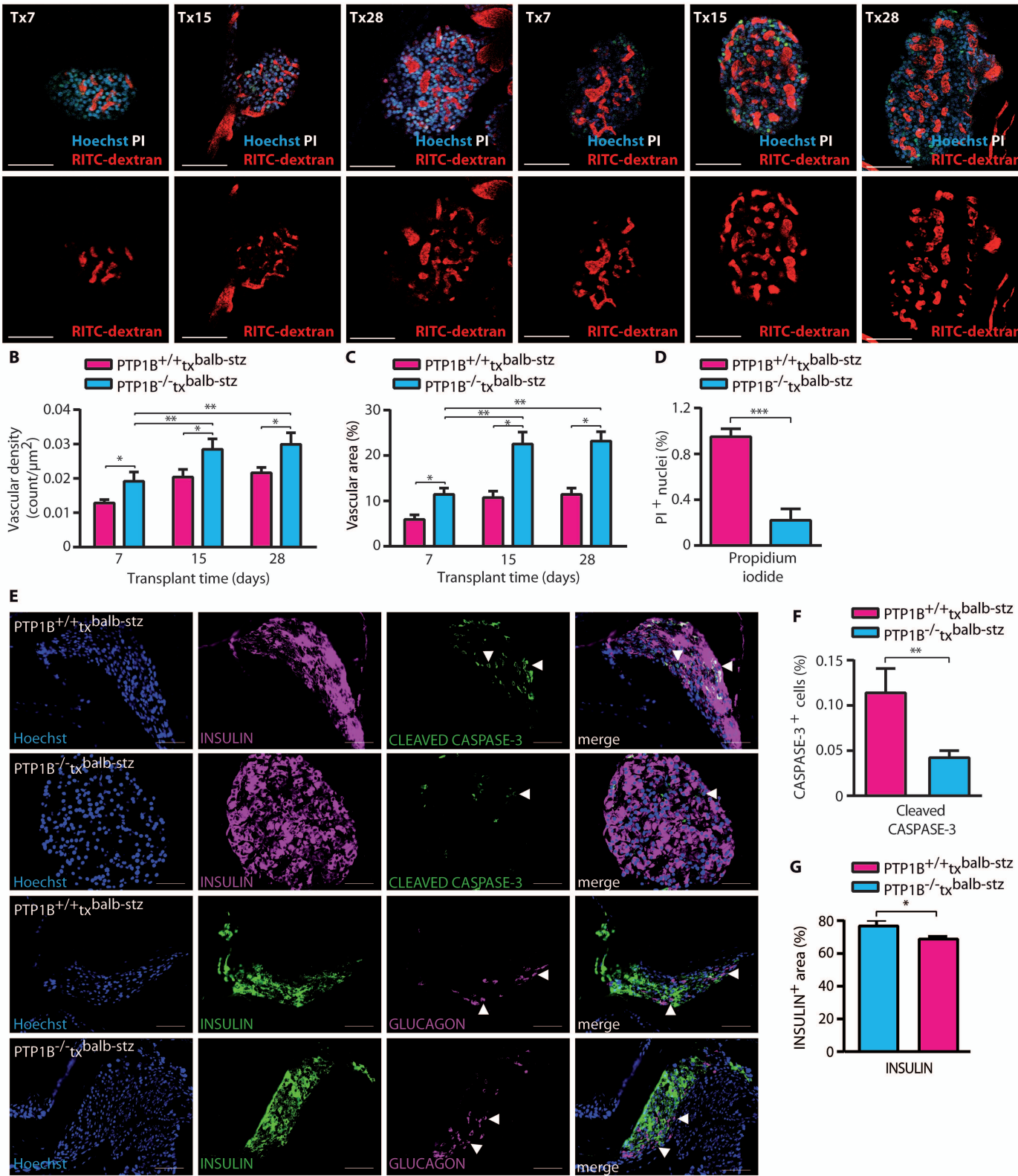
A
PTP1B+/+txbalb-stz
PTP1B-/-txbalb-stz
Tx7
Tx15
Tx28
Hoechst PI
RITC-dextran
RITC-dextran
B
PTP1B+/+txbalb-stz
PTP1B-/-txbalb-stz
Vascular density (count/µm2)
0.04
0.03
0.02
0.01
0
*
**
**
*
*
7
15
28
Transplant time (days)
C
PTP1B+/+txbalb-stz
PTP1B-/-txbalb-stz
Vascular area (%)
30
20
10
0
**
**
*
*
7
15
28
Transplant time (days)
D
PTP1B+/+txbalb-stz
PTP1B-/-txbalb-stz
PI + nuclei (%)
1.2
0.8
0.4
0
***
Propidium iodide
E
PTP1B+/+txbalb-stz
PTP1B-/-txbalb-stz
PTP1B+/+txbalb-stz
PTP1B-/-txbalb-stz
Hoechst
INSULIN
CLEAVED CASPASE-3
GLUCAGON
merge
F
PTP1B+/+txbalb-stz
PTP1B-/-txbalb-stz
CASPASE-3 + cells (%)
0.15
0.10
0.05
0
**
Cleaved CASPASE-3
G
PTP1B+/+txbalb-stz
PTP1B-/-txbalb-stz
INSULIN+ area (%)
80
60
40
20
0
*
INSULIN

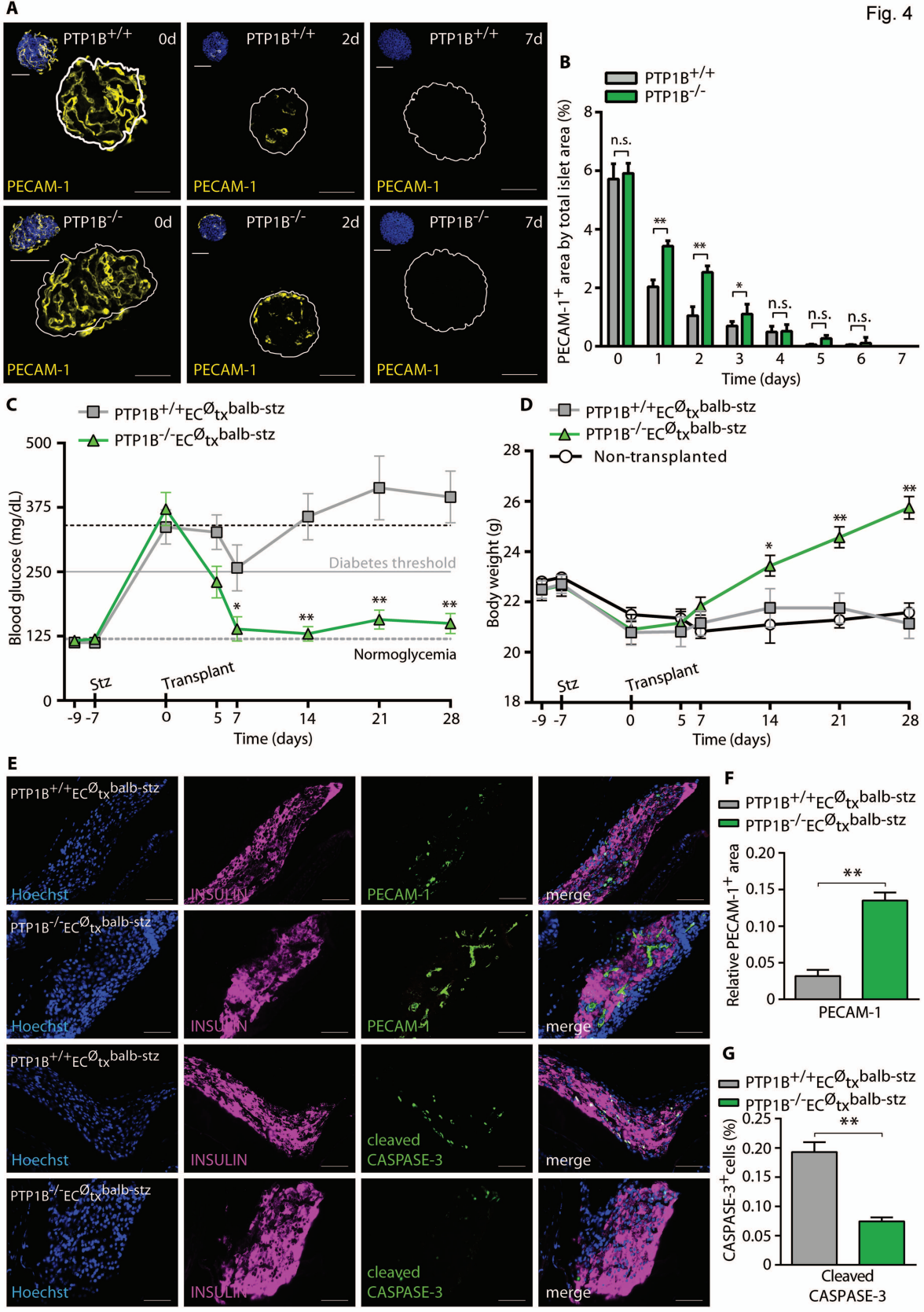
A
PTP1B+/+ 0d
PTP1B+/+ 2d
PTP1B+/+ 7d
PTP1B-/- 0d
PTP1B-/- 2d
PTP1B-/- 7d
PECAM-1
B
PTP1B+/+
PTP1B-/-
PECAM-1+ area by total islet area (%)
n.s.
**
*
Time (days)
C
PTP1B+/+ECØtxbalb-stz
PTP1B-/-ECØtxbalb-stz
Blood glucose (mg/dL)
Diabetes threshold
Normoglycemia
Stz
Transplant
Time (days)
D
PTP1B+/+ECØtxbalb-stz
PTP1B-/-ECØtxbalb-stz
Non-transplanted
Body weight (g)
Stz
Transplant
Time (days)
E
PTP1B+/+ECØtxbalb-stz
PTP1B-/-ECØtxbalb-stz
Hoechst
INSULIN
PECAM-1
merge
cleaved CASPASE-3
F
PTP1B+/+ECØtxbalb-stz
PTP1B-/-ECØtxbalb-stz
Relative PECAM-1+ area
PECAM-1
G
PTP1B+/+ECØtxbalb-stz
PTP1B-/-ECØtxbalb-stz
CASPASE-3+cells (%)
Cleaved CASPASE-3

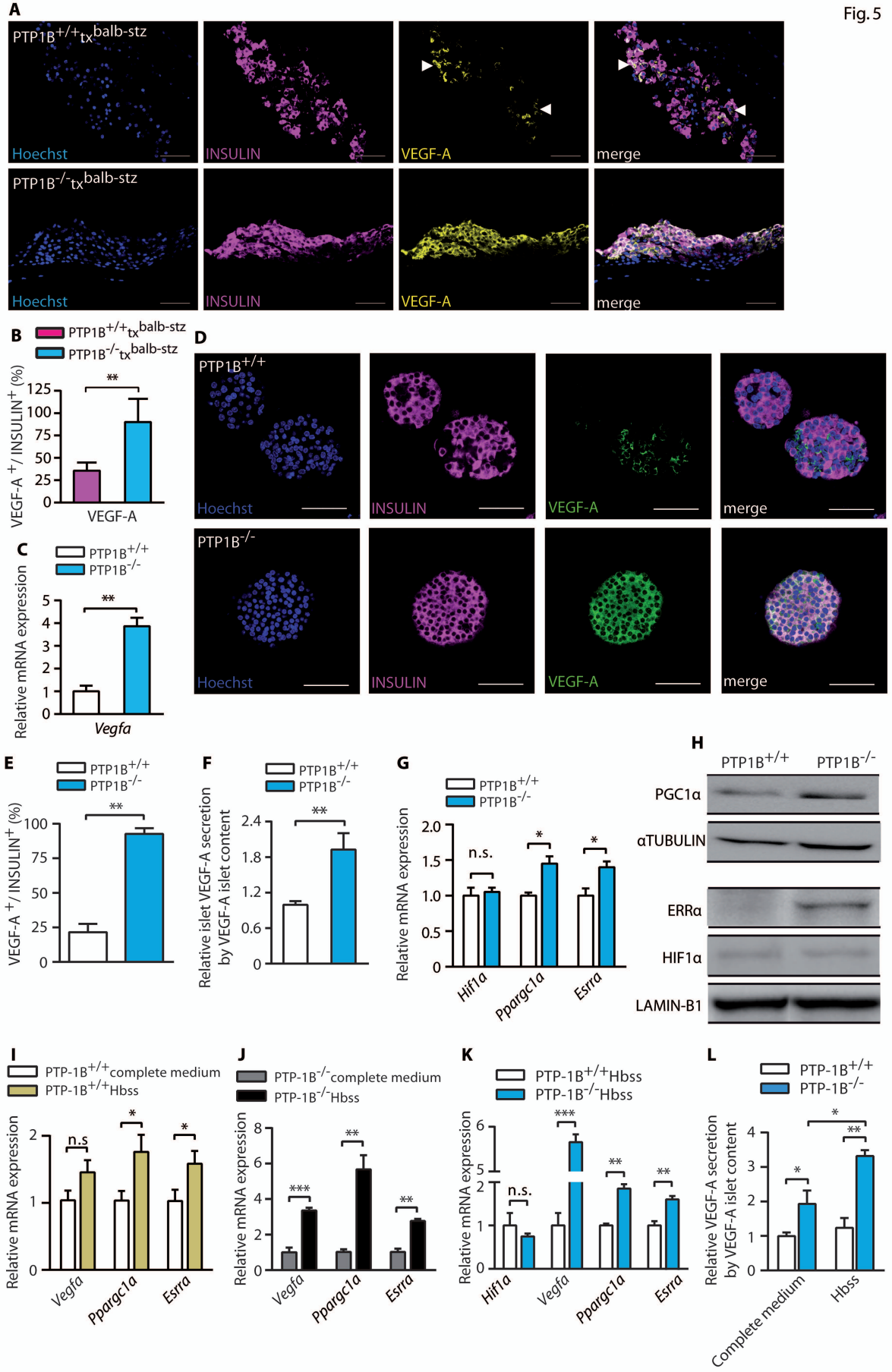
A
PTP1B+/+txbalb-stz
PTP1B-/-txbalb-stz
Hoechst
INSULIN
VEGF-A
merge
B
PTP1B+/+txbalb-stz
PTP1B-/-txbalb-stz
VEGF-A+/ INSULIN+ (%)
VEGF-A
C
PTP1B+/+
PTP1B-/-
Relative mRNA expression
Vegfa
D
PTP1B+/+
PTP1B-/-
Hoechst
INSULIN
VEGF-A
merge
E
PTP1B+/+
PTP1B-/-
VEGF-A+/ INSULIN+ (%)
F
PTP1B+/+
PTP1B-/-
Relative islet VEGF-A secretion by VEGF-A islet content
G
PTP1B+/+
PTP1B-/-
Relative mRNA expression
n.s.
Hif1a
Ppargc1a
Esrra
H
PTP1B+/+
PTP1B-/-
PGC1α
αTUBULIN
ERRα
HIF1α
LAMIN-B1
I
PTP-1B+/+complete medium
PTP-1B+/+Hbss
Relative mRNA expression
n.s
Vegfa
Ppargc1a
Esrra
J
PTP-1B-/-complete medium
PTP-1B-/-Hbss
Relative mRNA expression
Vegfa
Ppargc1a
Esrra
K
PTP-1B+/+Hbss
PTP-1B-/-Hbss
Relative mRNA expression
n.s.
Hif1a
Vegfa
Ppargc1a
Esrra
L
PTP-1B+/+
PTP-1B-/-
Relative VEGF-A secretion by VEGF-A islet content
Complete medium
Hbss

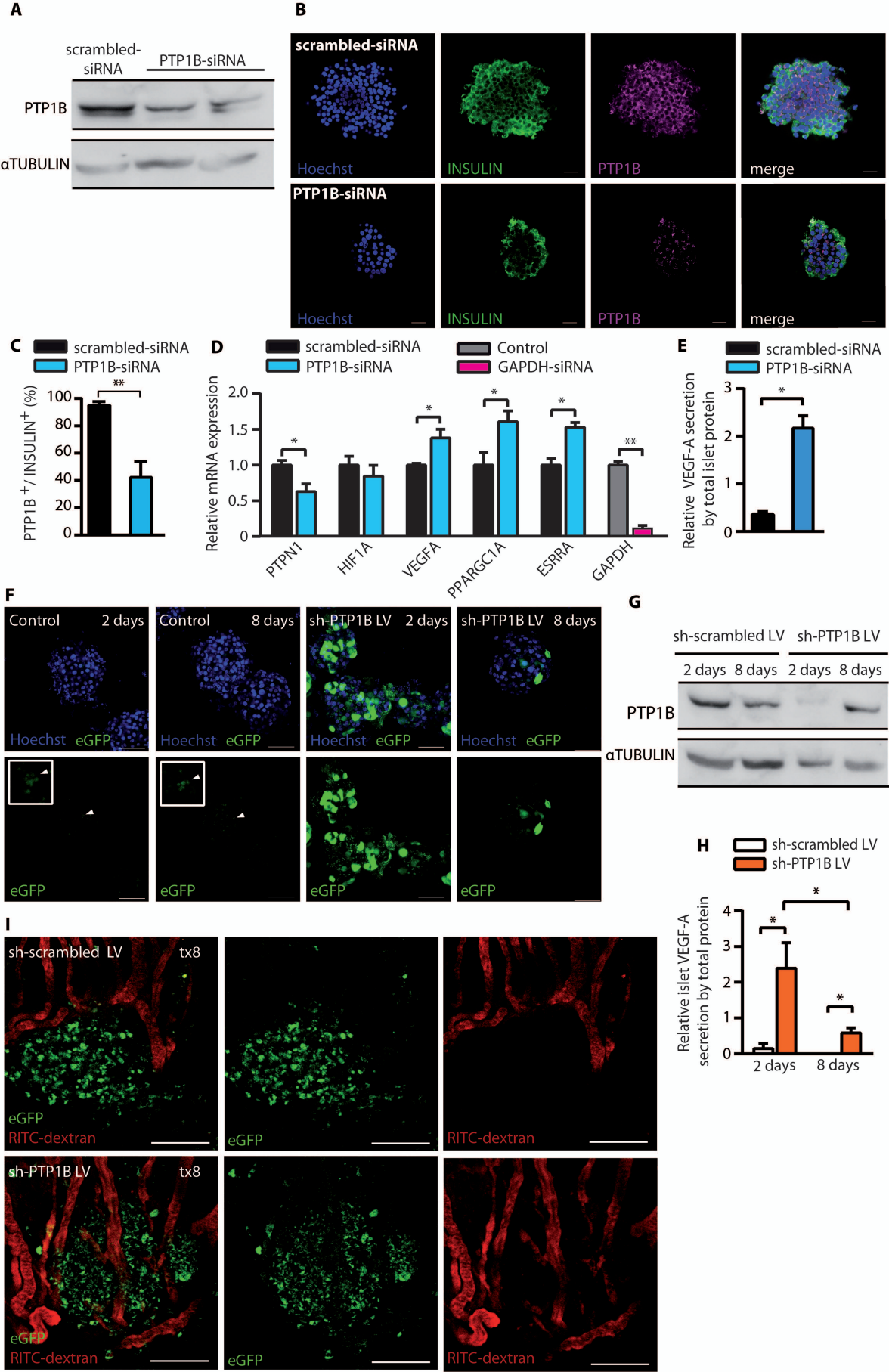
A
scrambled-siRNA
PTP1B-siRNA
PTP1B
αTUBULIN
B
scrambled-siRNA
Hoechst
INSULIN
PTP1B
merge
PTP1B-siRNA
C
scrambled-siRNA
PTP1B-siRNA
PTP1B+/INSULIN+ (%)
D
scrambled-siRNA
PTP1B-siRNA
Control
GAPDH-siRNA
Relative mRNA expression
PTPN1
HIF1A
VEGFA
PPARGC1A
ESRRA
GAPDH
E
scrambled-siRNA
PTP1B-siRNA
Relative VEGF-A secretion by total islet protein
F
Control 2 days
Control 8 days
sh-PTP1B LV 2 days
sh-PTP1B LV 8 days
Hoechst eGFP
eGFP
G
sh-scrambled LV
sh-PTP1B LV
2 days 8 days 2 days 8 days
PTP1B
αTUBULIN
H
sh-scrambled LV
sh-PTP1B LV
Relative islet VEGF-A secretion by total protein
2 days
8 days
I
sh-scrambled LV tx8
sh-PTP1B LV tx8
eGFP
RITC-dextran

Supplementary Materials

Supplementary Methods

Genotyping of PTP1b mice

Genotyping was performed by PCR on tail DNA using HotStarTaq DNA Polymerase (Qiagen, Hilden, Germany). The reaction was performed by denaturation at 95 °C for 15 minutes and 35 cycles of amplification (94 °C for 45 seconds, 53°C for 60 seconds, and 72 °C for 60 seconds), finishing with 5 minutes at 72 °C. Primers used were (5'-3'): GCGAGCTGTGGAAAAAAAAGG (PTP1B telomere repeat binding factors, Trf2), CGATCTCCTGCAATCCCTTC (PTP1B endogenous right #3, Erp3), CAGTCTTGGTCTACAGAGTG (PTP1B endogenous Left) and CCGCCTTTTCGCTAGCTGAC (PTP1B neo)

STZ-diabetes induction

Diabetes was induced in BALB/c mice through a single intraperitoneal injection of streptozotocin (STZ) 160 mg/kg at seven weeks of age*)*. Mice were fasted for four hours before streptozotocin administration, and fasting conditions were maintained 30 minutes after STZ administration. STZ (Sigma-Aldrich, Saint Louis, USA) was prepared under sterile conditions in a hood, due to its volatility. As STZ only maintains its stability and biological activity for 30 minutes in solution, we reconstituted STZ and prepared the corresponding dose immediately before the injection. STZ was reconstituted in cold 0.1M citrate buffer pH 4-5. Mice were followed for seven days, during which the non-fasting blood glucose was measured daily, on the same schedule, by collecting a drop of blood through the tail vein. Mice were considered diabetic

when having presented sustained blood glucose levels above 250 mg/dL for three consecutive days.

Mouse islet isolation

Mouse pancreatic islets were isolated by intraductal injection of ice-cold collagenase P (Roche Diagnostics GmbH, MHG, Germany) into the common bile duct. Collagenase P was reconstituted in cold Hank's balanced salt solution (Hbss, Sigma-Aldrich). The procedure causes collapse of the distal outlet of the common bile duct followed by an injection of collagenase in the proximity of the duct's cystic and hepatic ducts. After pancreas distention, a total pancreatectomy was performed and the pancreas was digested at 37°C in a bath with continuous gentle agitation. Digestion was stopped by adding ice-cold Hbss complemented with 0.1% bovine serum albumin (BSA). Islets were separated from the exocrine fraction by gradient centrifugation with Histopaque (Sigma-Aldrich) and further purified by islet handpicking under a stereoscopic microscope.

Islet transplantation

Immediately prior to transplantation, handcrafted blunted cannulas (0.4 mm internal diameter, Smiths Medical International, Hythe Kent, UK) were loaded with 200 islets and maintained at 37°C. Briefly, animals were anesthetized intraperitoneally with a mix of ketamine-xylazine (100 mg/kg and 7.5 mg/kg) and received a subcutaneous injection of buprenorphine (0.05 mg/kg) to alleviate postoperative pain. The animals were then transferred to a heat blanket placed under a stereoscopic microscope, in a sterile environment. An incision was made in the cornea near the corneoscleral junction, retracting the surrounding skin to facilitate access. The loaded cannula, connected to a 500 µL syringe, was introduced into the incision and the islets were carefully injected without damaging the iris. Finally, after the withdrawal of the cannula, a drop of

carboxymethylcellulose sodium (Allergan, Ireland) was administrated to the operated eye and the animals were placed under supervision in a warm environment until full recovery. All animals were followed for 28 days, maintaining normal light/dark cycle with food and water provided *ad libitum*.

Human islet batch purity and viability

To check batch purity, a random sample was stained with the zinc chelating-dye dithizone (DTZ). Zinc is mainly present in the ß-cell secretory granules coupled to insulin and DTZ produces bright red/pink islets when viewed by white-light microscopy *(64)*.

Assessment of islet viability was based on the evaluation of the islet cell membrane integrity using the fluorescent dyes carboxyfluorescein diacetate succinimidyl ester (CFDA, 10 μM) and propidium iodide (PI, 2.5 μg/mL). Whereas CFDA passively diffuses through the membrane of viable cells, PI enters cells that have compromised membranes binding to nucleic acids of the dying cells *(65)*. CFDA/PI fluorescence was assessed using the 488 nm and 532 nm lasers in a confocal Leica microscope. Dead cells (PI^+) were stained red and viable cells ($CFDA^+$) were stained green, both were quantified using the using ImageJ 1.50a. The islets were matched into categories: 0: few or no viable cells and the majority stained for PI (average viability=non-viable), 1: approximately 75% of the cells presented PI staining (average viability=25%); 2: approximately 50% of the cells with PI staining (average viability=50%); 3: approximately 25% of the cells were positive for PI (average viability=75%); 4: all cell viable (average viability=100%). To determine the total viability of the batch the following equation was used: Total viable=(0.25 (Σ of cat 1)+0.5 (Σ of cat 2)+0.75 (Σ of cat 3)+(Σ of cat 1)) 100 / total number of islets.

Gene expression analysis

The following mouse primers were used (forward (f) and reverse (r), 5'-3'):

Caspase3, (f) ATGGGAGCAGTCAG, (r) GTCCACATCCGTACCA;

Caspase9, (f) ATGCAGGGTGCGCCT,(r) GGTCTCAAGGTCTGTG;

Pecam1, (f) GCCTCACCAAGAGAACGGAAG, (r) GCTTTCGGTGGGGACAGGCTC;

Kdr, (f) CACTCTCCACCTTCAAACTCTC, (r) CTATTCCCCTTCCTCACTCTTC;

Cdh5, (f) TTGCCCTGAAGAACG, (r) ACTGCCCATACTTGAC;

Vegfa, (f) CACTTCCAGAAACACGACAAAC, (r) TGGAACCGGCATCTTTATCTC;

Hif1a, (f) CCCATTCCTCATCCGTCAATTA, (r) GGCTCATAACCCATCAACTCA;

Ppargc1a, (f) GCCGGAGCAATCTGAGTTAT, (r) GATCACCAAACAGCCGTAGA;

Esrra, (f) AAGTCCTGGCCCATTTCTATG, (r) CATCATGGCCTCAAGCATTTC.

The following human primers were used:

PTPN1, (f) GCTATGGTGAGGTGTGGATAAG, (r) AGCTCGCTACTTCTCTAACA;

HIF1A, (f) CCAGTTAGCTTCCTTCGATCAG, (r) GTAGTGGTGGCATTAGCAGTAG;

VEGFA, (f) CAGGACATTGCTGTGCTTTG, (r) CTCAGAAGCAGGTGAGAGTAAG;

PPARGC1A, (f) CCTTAAGTGTGGAACTCTCTGG, (r) CAGCTTTGGAGAAGCCTAA;

ESRRA, (f) TGCTGCTTAATCCTACC, (r) GCCCAATGCAAATGAGAG;

GAPDH, (f) AGGTCGGTGTGAACGGATTTG, (r) TGTAGACCATGTAGTTGAGGTCA;

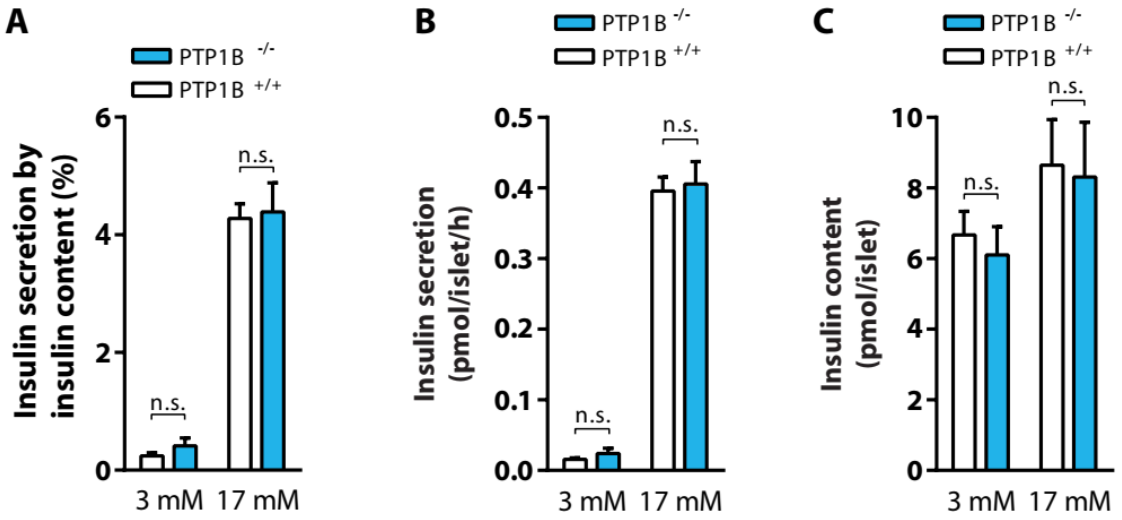

Fig. S1. In vitro glucose-induced insulin secretion by PTP1B$^{-/-}$ and PTP1B$^{+/+}$ mouse islets. Pancreatic islets, isolated from PTP1B$^{+/+}$ (white bars) and PTP1B$^{-/-}$ (blue bars) mice, were cultured for two days. After the two-day culture, glucose-induced insulin secretion was assessed by in vitro standard incubation assays. Secreted insulin and islet insulin content were measured by ELISA. Insulin secretion at glucose 3 mM and glucose 17 mM by PTP1B$^{+/+}$ (n = 6) and PTP1B$^{-/-}$ (n = 6) islets was expressed **(A)** relative to total islet insulin content or (**B**) amount of insulin secreted per islet. (**C**) Insulin content of the islet batches used in the static incubation assays. Bars represent mean ± s.d; n.s. not significant by Student's t-test.

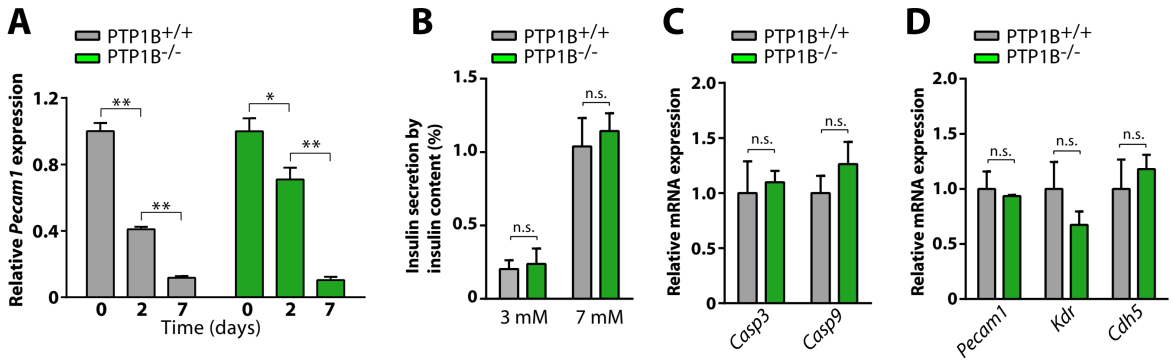

Fig. S2. Characterization of PTP1B$^{-/-}$ and PTP1B$^{+/+}$ mouse islets after seven days in culture. **(A)** Expression of *Pecam1* in PTP1B$^{+/+}$ (n = 9) and PTP1B$^{-/-}$ (n = 12) mouse islets at 0 (freshly-isolated), 2 and 7 days of culture. Values are expressed relative to day 0 islets. **(B)** In vitro glucose-induced insulin secretion (glucose 3 mM and glucose 17 mM) by seven-day cultured PTP1B$^{+/+}$ (n =4) and PTP1B$^{-/-}$ (n =4) mouse islets. Insulin secretion is expressed relative to islet insulin content (**C**,**D**) Expression of *Casp3*, *Casp9*, *Pecam1*, *Kdr*, and *Cdh5* in seven-day cultured PTP1B$^{+/+}$ (n = 5 and 7) and PTP1B$^{-/-}$ (n = 5 and 7) mouse islets. Data presented as mean ± SEM; n.s. not significant. *P < 0.05,**P < 0.01, by one-way ANOVA in (A,C,D)

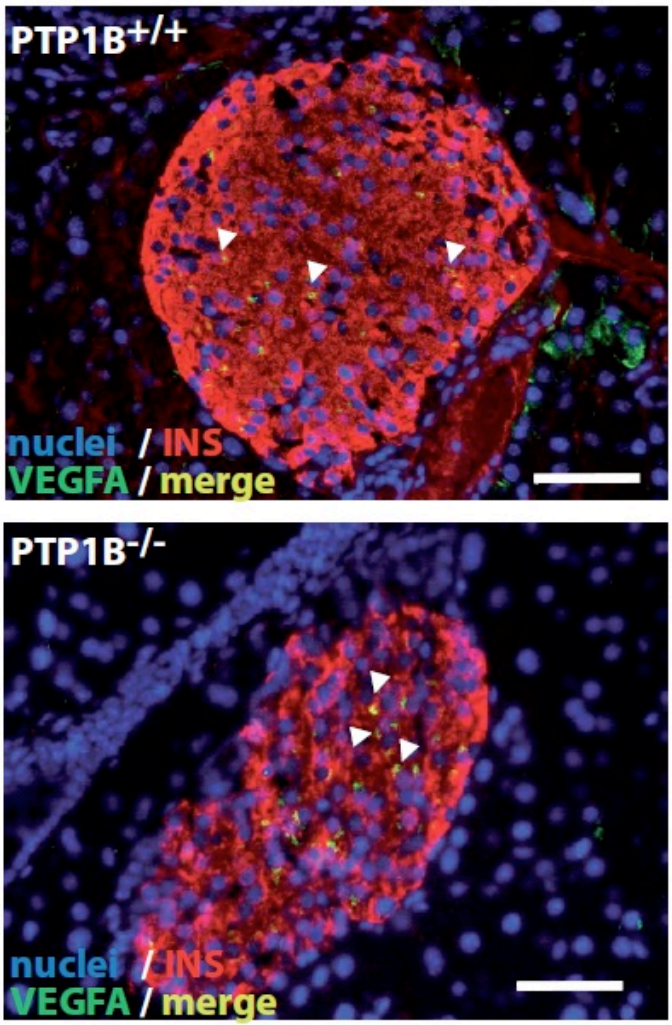

Fig. S3. Immunolocalization of VEGF-A in PTP1B$^{-/-}$ and PTP1B$^{+/+}$ mouse islets. Representative images of immunofluorescence staining for VEGF-A (green) and INSULIN (red) of native islets in paraffin-embedded sections of pancreases from PTP1B$^{+/+}$ (top) and PTP1B$^{-/-}$ (bottom) adult mice. White arrowheads indicate co-localization of VEGFA and INSULIN. Nuclei are marked with Hoechst (blue). Scale bars: 25 μm. Images representative of $n = 4$.

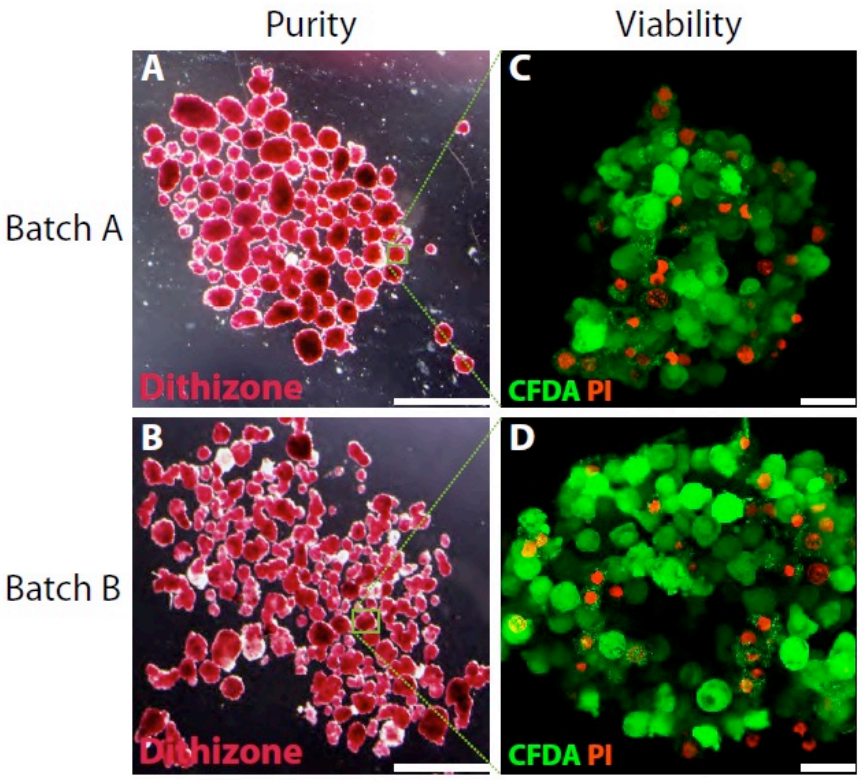

Fig. S4. Characterization of human islet preparations. (A, B) To determine batch purity aliquots of the human islets preparations were stained with the zinc-chelating agent dithizone, which selectively stains β-cells (pink) because of their elevated zinc content in the insulin secretory granules. Representative images of two human islet batches (left column, batch A, top; batch B, bottom). Scale bars: 1mm. (**C,D**) Batch viability was determined by membrane integrity staining using CFDA (viable cell marker, green) and PI (dead cells, nuclei staining, red). Representative maximum projection fluorescence images of islet batch A (top) and islet batch B (bottom). Images obtained using confocal microscopy. Scale bars: 15 µm.

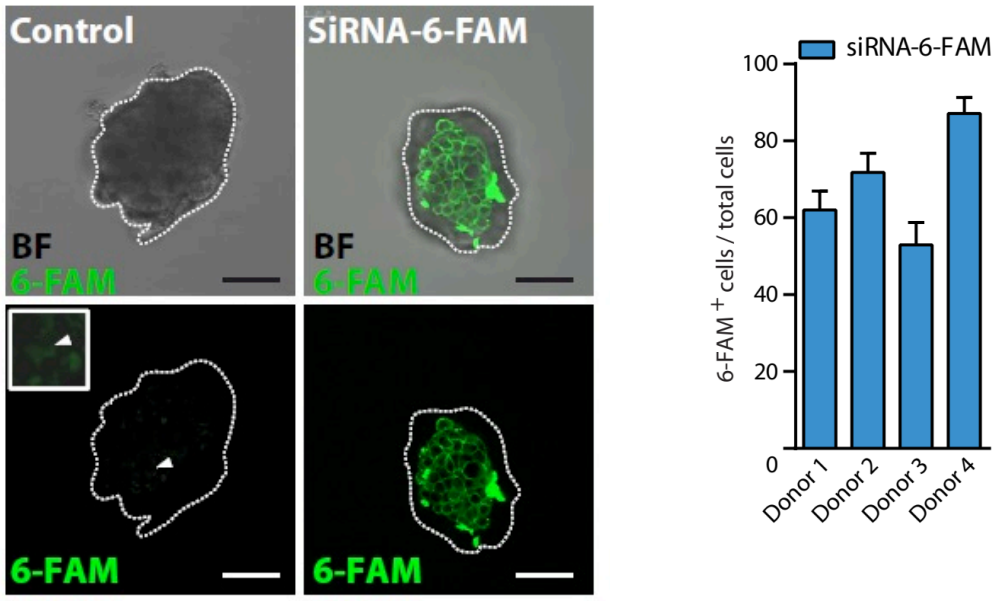

Fig. S5. Assessment of the uptake of siRNA by human islets. Human islets were transfected with a non-targeting siRNA coupled to 6-FAM (siRNA-6-FAM) or were left untreated (control). Representative images of bright field and 6-FAM fluorescence (n = 10 islets x 4 donors) obtained using confocal microscopy. On the right, graph depicts quantification of the percentage of 6-FAM$^+$ cells in four different islet donor preparations. Data represent mean ± SEM. Scale bars: 50 µm.

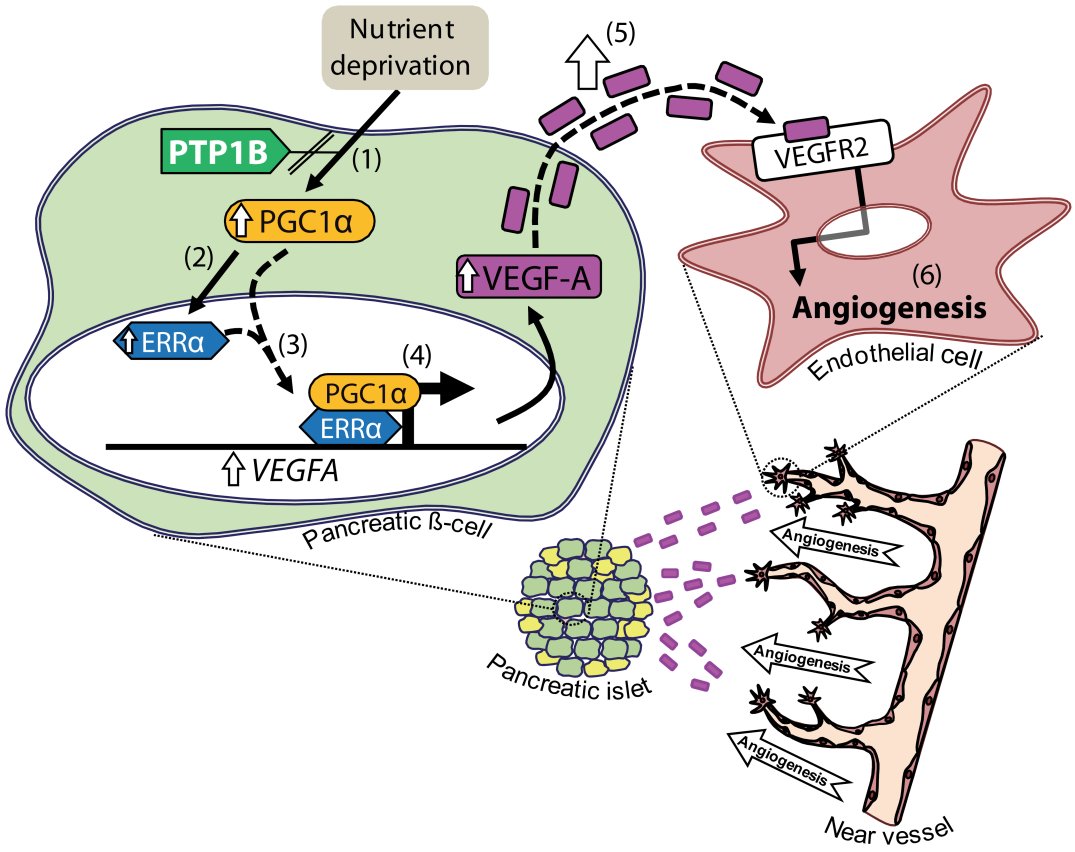

Fig. S6. Proposed model for the effect of PTP1B inhibition on islet graft vascularization.

Under conditions lacking a native vessel network (transplantation) and deficient in PTP1B, islet cells increase expression of PGC-1-ALPHA (1) and the orphan nuclear receptor ERR-ALPHA (2), which dimerize (3) and recognize several conserved sites at the *VEGFA* gene promoter (4), inducing the expression of this gene and leading to enhanced secretion of VEGF-A (5). VEGFA secreted by ß-cells interacts with its receptor, VEGFR2, in endothelial cells to induce graft angiogenesis (6).

Human islet preparation	1	2	3	4	5
MANDATORY INFORMATION					
Unique identifier	HM52	HM57	HM50	HM56	HM63
Donor age (years)	74	52	66	68	44
Donor sex (M/F)	F	M	M	M	F
Donor BMI (kg/m^2)	29,4	24,5	30,5	30,4	29,3
Donor blood glucose	11 mM	ND	9,9 mM	6,8 mM	8 mM
Donor HbA_{1c}	ND	ND	ND	ND	ND
Islet isolation centre	LTCD	LTCD	LTCD	LTCD	LTCD
Donor history of diabetes?	No	No	No	No	No

Table S1. Human islet donor information.

Donor characteristics of the five islet preparations used in this study. Human islets were isolated at the Laboratory of Cell Therapy for Diabetes (LTCD) at CHU de Montpellier and shipped to Barcelona to perform experiments.